Using a convection-permitting climate model to assess wine grape productivity: two case studies in Italy

Laura T. Massano[1], Giorgia Fosser[1], Marco Gaetani[1], Cécile Caillaud[2]

[1]Scuola Universitaria Superiore IUSS, Pavia, 2700, Italy
2Centre National de Recherches Météorologiques CNRM, Groupe de Météorologie de Grande Échelle et Climat

Correspondence to: Laura T. Massano (laura.massano@iusspavia.it)

Abstract. The article explores the potential use of climate models to reproduce wine grape productivity at local scale in Italy. To this end, both single and multiple regression approaches are used to link productivity data provided by two Italian wine consortia with bioclimatic indices. Temperature and precipitation-based bioclimatic indices are computed using the observational dataset E-OBS, the high-resolution climate reanalysis product SPHERA, the regional climate model CNRM-ALADIN and the km-scale convection-permitting climate model CNRM-AROME. The multiple regression method outperforms the single regression systematically, enhancing the ability of bioclimatic indices to explain productivity variability. The results show that productivity is strongly tied with temperature-based bioclimatic indices in the area of "Consorzio per la tutela del Franciacorta" in northern Italy, while for the "Consorzio del Vino Nobile di Montepulciano" area in central Italy both temperature and precipitation-based indices are relevant. Climate models, providing similar results as E-OBS and SPHERA, appear to be a useful tool to explain productivity variance. In particular, the added value of convection-permitting resolution is evident when precipitation-based indices are considered. This assessment shows windows of opportunity for using climate models, especially at convection-permitting scale, to investigate future climate change impact on wine production.

1 Introduction

Viticulture is tied to climate, that influences the suitability of an area, the yield and quality of wine grapes. The wine industry has a significant socio-economic influence and is a key agricultural sector in Italy. In 2022, Italy was the world's leading wine producer (49.8 million hl), and the second largest wine exporter, with a value of 7.8 billion euros (OIV, 2023). Over the coming decades, the wine sector is expected to be affected by climate change, especially in Italy that is part of the Mediterranean climatic hotspot (Giorgi, 2006; Tuel and Eltahir, 2020), where the impact of climate change is expected to be more severe than the global average. In this context, many studies investigated the impact of rising temperatures and changing rainfall patterns on grape growth (Bagagiolo et al., 2021; Bernetti et al., 2012; Gentilucci, 2020; Roehrdanz and Hannah, 2016; Sacchelli et al., 2017; Santillán et al., 2020). Since temperature is the primary driver for the phenological phases (Fraga et al., 2016), a warmer climate may lead to a shorter growing cycle and an earlier onset of phenological phases, which would increase frost-related

risk (Lamichhane, 2021; Trought et al., 1999). In fact, budburst is the most vulnerable phase to frost in the vine growing cycle, and an earlier budburst in spring would increase the exposure of the vine to late frost events. Furthermore, climate conditions typical of traditional wine-producing regions, such as Douro in Portugal, La Rioja in Spain, Bordeaux in France, and Tuscany in Italy, are expected to shift northwards or at higher altitude, and this modifications in viticulture suitability may consequently cause a decline in production (Adão et al., 2023; Rafique et al., 2023; Sgubin et al., 2023; Tóth and Végvári, 2016).

A common tool to investigate the impact of climate variability and change on the wine sector is the use of bioclimatic indices, defined from climate variables for specific plants and crops (Badr et al., 2018; Chou et al., 2023; Gaitán and Pino-Otín, 2023). A set of bioclimatic indices, based on temperature and heat accumulation (OIV, 2015), was proposed by the International Organisation of Vine and Wine (OIV), while precipitation-based indices were computed by (Badr et al., 2018) considering the research of Blanco-Ward et al., (2007). Bioclimatic indices are commonly used to assess a region's suitability for viticulture or zoning purposes, as well as in relation to phenology, harvest date and alcohol concentration (Dalla Marta et al., 2010; Koufos et al., 2014; Sánchez et al., 2019; Teslić, 2018). A novel application linking bioclimatic indices directly to wine grape productivity data in Italy was proposed by Massano et al., (2023) at regional level.

In Italy the vineyards are planted in extremely different areas, from the coasts to the hills, in some case also at considerable altitude (Tarolli et al., 2023). The wine production system is complex and fragmented, including both small farms and large companies. To valorise the designation of origin and guarantee a defined level of quality (Gori and Alampi Sottini, 2014; Ugaglia et al., 2019), producers are organized in wine consortia (Consorzi di Tutela) according to the EU and national regulations, i.e. Regulation (EU) No 1308/2013. To address this fragmentation and account for the typicity of the wine business (Agnoli et al., 2023; Spielmann and Charters, 2013), yield data from wine consortia and high-resolution climate data are of prominent importance for local-scale impact studies and, thus for effective adaptation strategies.

In the context of impact studies at local scale, requiring high-resolution climatic data, the use of km-scale convection permitting models (CPM) is increasing (Bamba et al., 2023; Le Roy et al., 2021; Tradowsky et al., 2023). Due to their high spatial resolution (less than 4 km), CPMs can represent convection explicitly, without using the parameterisation of deep convection, and thus reduce the model uncertainty (Fosser et al., 2024). Compared to coarser resolution regional climate models (RCMs), the CPMs represent more realistically hourly rainfall intensity, the diurnal cycle of precipitation and the extremes and are thus consider more reliable in terms of climate projections of precipitation (Ban et al., 2021; Brisson et al., 2016; Coppola et al., 2020; Fosser et al., 2020; Kendon et al., 2017; Pichelli et al., 2021). The advantages of CPMs versus RCMs has been also explored in the assessment of the impact of climate change on agriculture and crop production (Agyeman et al., 2023; Berthou et al., 2019; Chapman et al., 2020, 2023). Nevertheless, no prior studies have employed CPMs to examine the influence of climate variability and change on viticulture.

The present study presents a novel approach to estimate wine grape productivity at the local scale by using a CPM, showing windows of opportunity for the use of CPMs in the context of ongoing and future climate change. The impact of climate variability on wine grape productivity are investigated by relating temperature and precipitation-based bioclimatic indices to wine productivity data provided by two wine consortia in northern and central Italy. The CPM performance is validated against

climate observations and a km-scale reanalysis product. Furthermore, the added value of the higher resolution is assessed by comparing the CPM to an RCM simulation. Single and multiple regression approaches are used to determine to which extent bioclimatic indices can explain changes in wine grape productivity at local scale. The multiple regression approach accounts for the potential interplay between the bioclimatic indices, potentially increasing the portion of total productivity variability explained by the individual indices, as found by Massano et al., (2023).

2 Data and Methods

2.1 Wine grape productivity data

Wine grape yield data, as well as the hectares of vines, are collected from two wine consortia in Italy: 'Consorzio per la tutela del Franciacorta' (FRA) and 'Consorzio Del Vino Nobile di Montepulciano' (MON). The first one lies in Franciacorta, a small (200 km2) wine-growing region in Lombardia (LOM), in northern Italy, mostly known for sparkling wine (Figure 1). The area is characterised by a humid subtropical climate according to the Koppen classification (Costantini et al., 2013). The Iseo lake, located at the northern border of this region, is the sixth largest lake in Italy and tempers the typical heat of the plain in summer, while in winter protects the vineyards from the freezing air arriving from the north (Leoni et al., 2019). The consortium was born in 1990 as a result of the endeavour of local producers that felt the need to preserve the original production method of the Franciacorta wine. Today the consortium is composed by 200 winemakers and preserves three designations: Sebino IGT (Typical Geographical Indication), Franciacorta DOCG (Denomination of Controlled and Guaranteed Origin) and Curtefranca DOC (Denomination of Controlled Origin), known as “Terre di Franciacorta” before 2011 (https://franciacorta.wine/en/). This analysis focuses on the designations of Franciacorta DOCG and Curtefranca DOC available from 1997 to 2019 (23 years), discarding Sebino IGT, for which data are only available for a limited period.

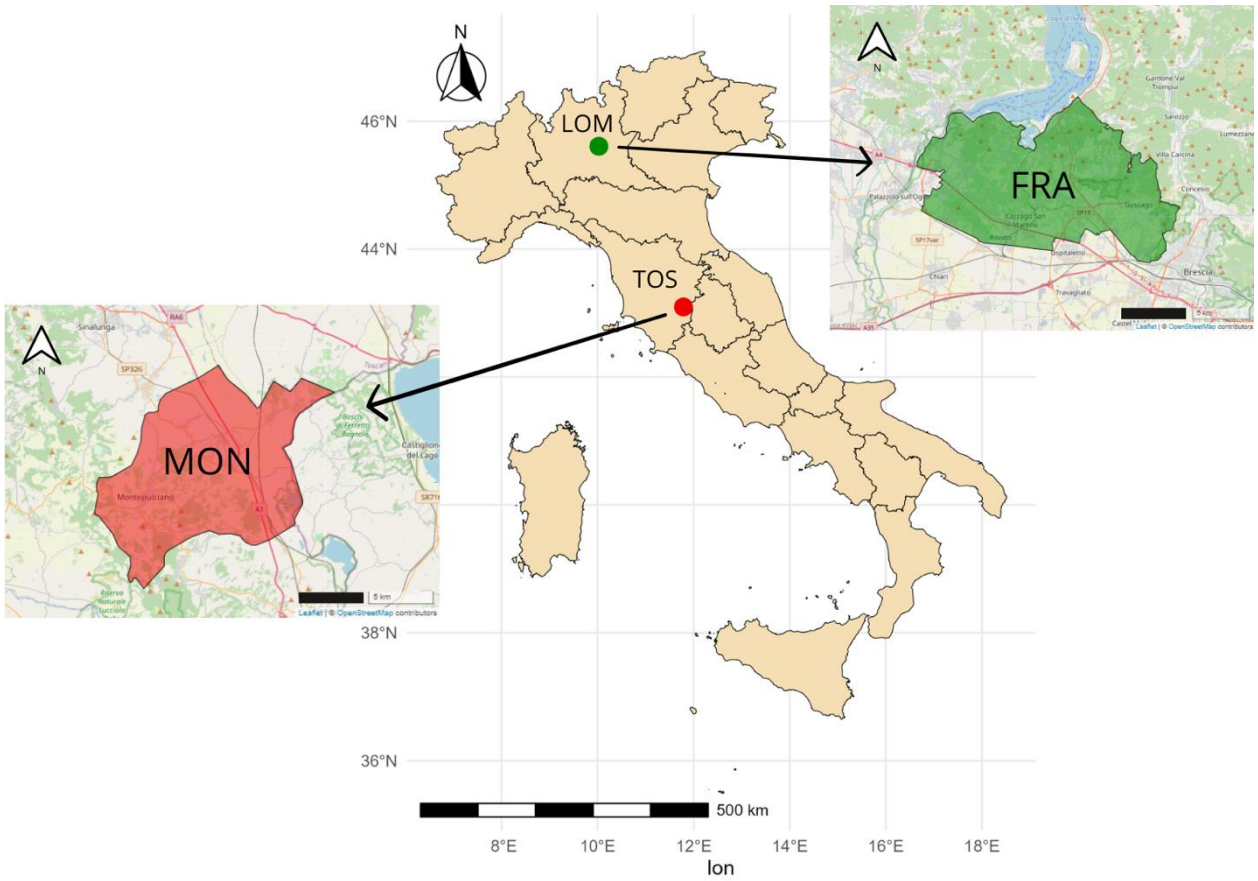

Figure 1: Map of Italy highlighting in green the area of Franciacorta Consortium (FRA) in the Lombardia (LOM) region, and in red the area of the Consorzio del Vino Nobile di Montepulciano (MON) in the Toscana (TOS) region (base layer : © OpenStreetMap contributors 2019. Distributed under the Open Data Commons Open Database License (ODbL) v1.0.).

The "Consorzio del Vino Nobile di Montepulciano" (MON) (https://www.consorziovinonobile.it/) is located within the Montepulciano territory in Toscana (TOS) region in the centre of Italy (Figure 1). The area is characterized by a Mediterranean climate with hot and dry summer, and mild and rainy winters (Costantini et al., 2013). The consortium preserves three designations, namely Vino Nobile di Montepulciano DOCG, Rosso di Montepulciano DOC and Vin Santo di Montepulciano DOC. The study focuses on the first two designations that have the longest time series covering 31 years between 1989 and 2019.

For each wine designation, the FRA consortium directly reports the quantity of grapes harvested in quintals (q), while MON indicates the hectolitres of wine produced (hl) and the maximum percentage of grape yield convertible into wine (70%). For the analysis, the hectolitres are converted into quintals using the maximum percentage allowed, and then the productivity (q/ha) is calculated by dividing the quintals of grapes by the vineyard area.

To assess the consistency of productivity data between local and regional scales, the productivity at the local scales (FRA and MON) is compared with productivity at regional scale provided by the Italian National Institute of Statistics (ISTAT). ISTAT provides data of harvested wine grape (in quintals) and vintage area (in hectares) from 1980 onwards. However, the data are not homogenous over time in terms of spatial aggregation. Wine grape productivity data are available at the provincial level between 1980 and 1993 and from 2006 to 2019; at the regional level between 1994 and 2000; at the national scale from 2000 to 2005. Following Massano et al. (2023), the data were aggregated at regional level for Lombardia (LOM) and Toscana (TOS) region, where the FRA and MON consortia are respectively located, for the period 1980–2019, with a six-year gap between 2000 and 2005. Considering the overlapping periods between ISTAT and consortia time series, it is found that the regional and local productivity data are significantly correlated ($p<=0.05$) for both FRA and MON (Table A 1). In addition, the application of a Welch's *t*-test, designed to assess whether two samples are extracted from the same population, proves that the productivity distributions of both consortia are consistent with the respective regional productivity distributions (Table A 1 and Figure A 1).

2.2 Climate observations and reanalysis data

The observational dataset used is E-OBS, a gridded daily dataset covering Europe from January 1950 to the present day. E-OBS is constructed using data from the meteorological stations provided by the European National Meteorological and Hydrological Services or other data holding institutions (Photiadou et al., 2017; Van Der Schrier et al., 2013). The analysis is based on the latest available version (v28) at 0.1 deg (~11 km). Although the E-OBS database is frequently used to validate climate models (Christensen et al., 2008; Jaeger and Seneviratne, 2011; Lorenz and Jacob, 2010; Retalis et al., 2016), some studies have pointed out some limitations in the E-OBS representation of precipitation and temperature, mainly due to the inhomogeneity of the station network used for interpolation (Kyselý and Plavcová, 2010; Liakopoulou and Mavromatis, 2023; Van Der Schrier et al., 2013).

In addition to observations, the analysis uses a high-resolution convection-permitting reanalysis product, called SPHERA (High rEsolution ReAnalysis over Italy; Cerenzia et al., 2022; Giordani et al., 2023), produced by ARPAE-SIMC (Agency for Environmental Protection of the Emilia Romagna Region, Italy). Based on the non-hydrostatic limited-area model COSMO (Baldauf et al., 2011; Schättler et al., 2018), SPHERA dynamically downscales the global reanalysis ERA5 (Hersbach et al., 2020) boundary condition, updated every hour, in sequence of 24-h-long integrations. Being a reanalysis product, SPHERA assimilates in situ observations using a continuous nudging approach based on the Newtonian relaxation principle (Stauffer and Seaman, 1990). The quality-checked observational data nudged in SPHERA are wind speed components, pressure, air humidity, and temperature (excluding 2m temperature) derived from ECMWF catalogue, i.e. SYNOP, SHIP, TEMP, PILOT and AIREP. More details on the SPHERA configuration can be found in Cerenzia et al., (2022). This new reanalysis product covers Italy at a horizontal resolution of 2.2 km with a temporal coverage of 26 years (1995-2020). When validated against independent rain gauge observations, SPHERA showed an improved representation of the precipitation field, both at daily and hourly scales, compared to its driver, i.e. ERA5 (Giordani et al., 2023). The performance of SPHERA demonstrates that it can

be a valuable resource for improving climate monitoring by providing insights into regional climate change impacts (Giordani et al., 2023). The SPHERA data, provided at hourly time steps, have been aggregated at the daily time scale for the purpose of this study.

In this study, the E-OBS dataset and SPHERA reanalysis are both employed as a reference. This strategy enhances the validation process and evaluate the potential of a reanalysis product to serve as an alternative to observation for the validation of climate models as well as for viticulture studies.

2.3 Climate model data

The French Centre National de Recherches Météorologiques (CNRM) provides two climate simulations spanning the period 2000-2018. The first simulation, covering the Med-CORDEX domain (Ruti et al., 2016) at 12.5 km resolution, is performed with the RCM CNRM-ALADIN (Nabat et al., 2020), the limited area version of ARPEGE-Climate global model, driven every 6 hours by the ERA-Interim (80 km) reanalysis (Dee et al., 2011). The second one is performed with the CPM CNRM-AROME, driven by the CNRM-ALADIN simulation every hour, and covers with a resolution of 2.5 km the pan-Alpine domain defined within the CORDEX FPS on Convection programme (Coppola et al., 2020; Lucas-Picher et al., 2023). In contrast with any reanalysis datasets (e.g., SPHERA), climate models do not assimilate observations. This has the disadvantage to lead usually to larger biases than reanalysis (at least for variables which are assimilated in the reanalysis), but the advantage that they can be used for climate projections. The main difference between CNRM-ALADIN and CNRM-AROME resides in the parameterisation of deep convection, which may be source of errors and uncertainty (e.g., Prein et al., 2015), active in the former and switch off in the latter. In addition, CNRM-AROME, being a kilometre-scale model, allows a more accurate representation of surface and orographic features. Both models have been extensively evaluated (e.g. Ban et al., 2021; Coppola et al., 2020; Daniel et al., 2019; Fumière et al., 2020; Nabat et al., 2020; Pichelli et al., 2021). In particular, Caillaud et al., (2021) found that the CNRM-AROME, besides an underestimation of the highest intensities, realistically represents autumn extreme precipitation at both daily and hourly timescale in terms of location, intensity, frequency and interannual variability, while CNRM-ALADIN fails to do so. Both CNRM-ALADIN and CNRM-AROME (hereafter simply called respectively RCM and CPM) provide hourly output, which are aggregated at the daily time scale for the purpose of this study.

2.4 Validation of climate simulations

In this work, temperature and precipitation data from the observational dataset E-OBS, the climate reanalysis product SPHERA and the climate model simulations, at regional (RCM) and convection-permitting scale (CPM), are used for the calculation of a set of bioclimatic indices described in the next section. The analysis focuses on the 19 years from 2000 to 2018 that is the longest period available for RCM and CPM simulations and shared with E-OBS, SPHERA climate data and FRA and MON productivity data. To compare datasets with different horizontal resolutions on equal terms (Berg et al., 2013), observations, reanalysis and model simulations are conservatively remapped on a common grid, i.e. the E-OBS regular grid at ~11 km, the

coarsest among all. Tests performed to assess the impact of upscaling SPHERA and CPM at a coarser resolution showed no significant changes in the results (not shown).

Then, the climatic variables (i.e. P: Precipitation; TM: mean temperature, TX: max temperature and TN: min temperature) are retained on all available grid cells within the areas of interest (LOM and TOS). Subsequently, the consortium territory is cropped using the respective shape files of FRA and MON. Finally, the spatial average is calculated by weighting the contribution of each grid cell according to the percentage of the cell falling within the consortium territory. The shape file of the FRA consortium's territory is provided directly by the consortium's technical office, while the shape file for MON is created by selecting the municipality listed in the appellation regulation for the relevant denominations (i.e., Montepulciano municipality).

The precipitation and temperature timeseries of the climate simulations are analysed against the observational datasets (i.e. E-OBS and SPHERA) to evaluate the biases in the climatic conditions in the region of interest, prior to examine the bioclimatic indices. In particular, the CPM performance is evaluated for the period 2000-2018 against both SPHERA and E-OBS and compared to the RCM. In this study, the new SPHERA reanalysis product is used as a reference dataset together with the E-OBS dataset, which is already widely used for model validation (Kyselý and Plavcová, 2010). The comparison between climate model simulations and the reference datasets is carried out by computing the Spearman correlation, the Root Mean Square Error (RMSE) and the Normalised Root Mean Square Error (NRMSE) with respect to the range of values, i.e. the maximum value of the variable considered (y_{max}) minus the minimum value (y_{min}), for the reference datasets (SPHERA and E-OBS). In particular, the Spearman correlation coefficient is used to assess the ability of the climate models in reproducing the climate variability of the reference datasets, while RMSE and NRMSE provides a measure of the climate models biases. Moreover, the statistical significance of the model biases is assessed by applying a Welch's two-tailed t-test (Welch, 1938), with a 95% level of confidence.

2.5 Bioclimatic indices

This study considers ten bioclimatic indices (summarised in Table 1), computed following the same methodology previously described for the climate variable. Eight of theme, recommended by the International Organisation of Vine and Wine (OIV) are based on temperature and heat accumulation, while the remaining two are based on rainfall accumulation.

The temperature-based indicators are:

1. Daily mean temperature during vegetation period (TmVeg) calculated between 1st April to 31st October (Jones et al., 2005). Temperature in spring plays a key role in determining the timing of the phenological events, as underlined by Malheiro et al., (2013). In general, higher TmVeg leads to an anticipation of the phenological phases, while TmVeg values above 24 °C or below 12 °C are considered unfavourable to wine-growing (Eccel et al., 2016).

2. Heliothermic Huglin index (HI), which is calculated by summing, when positive, the average between the mean and the maximum temperature, in relation to the baseline temperature of 10°C i.e. the physiological threshold for the start of the vine growth cycle (Huglin M, 1978; Teslić, 2018), over the period from 1st April to 30th September and corrected by a coefficient of day duration. The HI index is tied to vine growing and grape sugar concentration with higher HI leading to an increased vine vigour and higher sugar content in the grapes. According to (Tonietto and Carbonneau, 2004), a climate with a heat index (HI) of more than 3000 degree days (GDD) is classified as 'very warm', while below 1200 degree days is “too cold”. Both these situations are associated to plant stress and thus lead to a production reduction.

3. Winkler degree days (WI), which provides a measure of heat accumulation during the growing season, is the sum of daily mean temperatures above 10°C from 1st April to 31st October (Amerine and Winkler, 1944; Piña-Rey et al., 2020). Similarly, to HI, WI index is linked to the rate of growth of the vines and the development of the fruits, with values between 850 and 2700 degree days being optimal for the wine production (Eccel et al., 2016).

4. Biologically Effective Degree Days (BEDD), which is the sum of daily mean temperatures in the range between 10 °C and 19 °C, from 1st April to 31st of October. The BEDD index uses the same baseline temperature (10 °C) as WI and HI indices but also takes into consideration that vine growth is unlikely to occur above the upper temperature threshold of 19°C (Anderson et al., 2012; Gladstones, 1992). As the previous temperature-based indices, too high (above 2000 degrees per day) or too low (below 1000 degrees per day) values of BEDD can potentially reduce productivity.

5. Cool Night Index (CNI), defined as the average of minimum air temperatures during the month of September. Low minimum temperatures in September increase the polyphenolics in the grapes and are beneficial for the overall quality of the harvest (Tonietto and Carbonneau, 2004). Although CNI is more related to grape quality than quantity, Massano et al (2023) found that this index can help explaining changes in productivity especially when used in combination with other bioclimatic indices.

6. Minimum temperature during vegetative period (TnVeg), which is the minimum temperature recorded during the vegetative period (1st April to 31st October). This index is important to assess whether the vines are exposed to low temperature or even to spring frosts that pose a significant risk to viticultural practices and production. The damage threshold is fixed at -2 °C (Sgubin et al., 2018).

7. Maximum temperature during vegetative period (TxVeg), which is the maximum temperature recorded during the vegetative period. This index is useful for assessing the occurrence and the severity of summer hot-spells that can damage to vineyard, thus reducing the wine productivity (Cabré and Nuñez, 2020). The heat stress threshold is set at 35°C, above which physiological damage to the vines is expected (Hunter and Bonnardot, 2011).

8. Minimum temperature during rest period (TnRest), defined as the minimum temperature during rest period, i.e. 1st November to 31st March. This index is used to determine winter severity. Grapevines can tolerate temperatures as -25 °C (Düring, 1997; Lisek, 2012), although damage can already occurs at -15 °C (Eccel et al., 2016)

The indices based on precipitation are:

1. Growing season precipitation index (GSP), defined as rainfall accumulated from 1st April to 30th September and used to assess the water stress for non-irrigated grapevines (Blanco-Ward et al., 2007; Piña-Rey et al., 2020), as in Italy where irrigation is only allowed in extreme cases (e.g., long drought periods).

2. Spring Rain index (SprR), which measures the amount of rain accumulated between the 21st of April and the 21st of June (Raül Marcos-Matamoros et al., 2020). This indicator of spring wetness can be related to production. In fact, while dry springs can delay vegetative growth, wet ones can increase plant vigour but also lead to a higher risk of fungal diseases (Dell'Aquila, 2022).

Table 1: Acronyms and formulas of the bioclimatic indices used.

	Definition	Formula	Suitable class range
Temperature-based	Mean temperature during vegetation period (TmVeg)	$TmVeg = T_{mean}$ (1) $between\ 1st\ April\ and\ 31th\ October$	13-24 °C (Eccel et al., 2016)
	Heliothermic Huglin index (HI)	$HI = K \sum_{01Apr}^{30Sep} max\left[\left(\frac{(T_{mean}-10)+(T_{max}-10)}{2}\right); 0\right]$ (2) K=1.04 length of days coefficient	1200-3000 GDD (Tonietto and Carbonneau, 2004)
	Winkler degree days (WI)	$WI = \sum_{01Apr}^{31Oct} max\left[\left(\frac{T_{min}+T_{max}}{2} - 10\right); 0\right]$ (3)	850-2700 GDD (Eccel et al., 2016)
	Biologically Effective Degree Days (BEDD)	$BEDD = \sum_{01Apr}^{31Oct} min\{max\left[\left(\frac{T_{min}+T_{max}}{2} - 10\right); 0\right]; 9\}$ (4)	1000-2000 GDD (Gladstones, 1992)
	Cool Night Index (CNI)	$CNI = \frac{1}{30}\sum_{01Sep}^{30Sep} T_{min}$ (5)	12-18 °C (Tonietto and Carbonneau, 2004)
	Minimum temperature during vegetative period (TnVeg)	$TnVeg = T_{min}\ between\ 01\ Apr\ and\ 31\ Oct$ (6)	Damage threshold -2 °C (Sgubin et al., 2018)
	Maximum temperature during vegetative period (TxVeg)	$TxVeg = T_{max}\ between\ 01\ Apr\ and\ 31\ Oct$ (7)	Upper threshold 35 °C (Hunter and Bonnardot, 2011)
	Minimum temperature during rest period (TnRest)	$TnRest = T_{min}\ between\ 01\ Nov\ and\ 31\ Mar$ (8)	Above -25 °C (Düring, 1997; Lisek, 2012)
Precipitation-based	Growing season precipitation index (GSP)	$GSP = \sum_{01Apr}^{30Sep} Prec$ (9) *Prec: total precipitation*	200-600 mm (Badr et al., 2018)

	Spring Rain index (SprR)	$SprR = \sum_{21Apr}^{21Jun} Prec$ (10)	(Dell'Aquila, 2022)

The bioclimatic indices computed using climate simulations (RCM and CPM) are analysed against the observational datasets (E-OBS and SPHERA) following the same methodology described for the climatic variables (i.e. P: Precipitation; TM: mean temperature, TX: max temperature and TN: min temperature).

2.6 Trend Analysis

A trend analysis for both the climatic variables and the bioclimatic indices is performed to assess the evolution of the climatic condition in FRA and MON in the period 2000-2018; the same analysis is also carried out for productivity data. The presence and the magnitude of trends are determined using respectively the non-parametric Mann-Kendall test and the Sen's slope method, with a significance level of 95% (Hanif et al., 2022; Mann, 1945). The Sen's slope estimator calculates the rate of change over time of a variable by taking the median of the slopes of all linear regressions between points pairs (Aswad et al., 2020). The assessment of possible trends aims to investigate whether the long-term component of variability may be dominant over the interannual component.

2.7 Single and multiple regression approach

The Spearman correlation coefficient between each bioclimatic index and the wine grape productivity is calculated for both consortia area and the threshold for statistical significance is set to 95%. This analysis aims at assessing the fraction of wine grape productivity variability explained by the bioclimatic indices and the ability of climate models to represent this relationship compared to the observational datasets.

Furthermore, a multiple regressive (MR) approach is applied to determine whether a linear combination of indices can enhance the total productivity variability explained by the bioclimatic indices (Massano et al., 2023). The *best-subset selection* approach, implemented by (James G et al., 2013), is used to optimise the prediction of productivity, as in Massano et al. (2023). This approach seeks the subset of predictors, i.e. the bioclimatic indices in this case, that most accurately predicts the predictand, i.e., the productivity, by examining all feasible predictor combinations and thus selecting the one minimising the error in the prediction. This is achieved by utilising the k-fold cross-validation method. The k-fold cross validation method is employed to identify the optimal model (Kassambara, 2018). This method performs cross-validation by randomly dividing the data into k subsets of approximately equal size, with k typically set to 5 or 10 (here k = 5 is used). One of the folds serves as test set and the remaining as training set. This process is repeated k times, whereby varying groups of data are utilized as training or testing sets. Subsequently, the mean squared error is computed. The average of the mean squared errors of all iterations is the model prediction error (CV - cross validation error) (James et al., 2021; Kuhn and Johnson, 2013; Wassennan, 2004). The performance of the multi regressive model is assessed by the adjusted R-squared coefficient of determination

(AdjR^2), while the p-value is used to determine statistical significance at 95% level. The so-optimised MR model (productivity = $_1$*index$_1$ + a_2*index2 + a_3*index$_3$ + …, with index$_n$ indicating the selected bioclimatic index) is then used to predict the productivity and the Pearson correlation between predicted and observed productivity is calculated. Following Massano et al. (2023), the comparison between the SR and MR methods is performed in terms of the productivity variance explained by the prediction, estimated by computing the coefficient of determination, i.e. the square of the correlation coefficient.

3 Results

3.1 Validation of the climate simulations

Prior to the computation of the bioclimatic indices, the precipitation and temperature fields in both consortia (FRA and MON) are analysed to assess the potential biases, which could impact on the temperature and precipitation-based bioclimatic indices. Figure 2 for FRA and Figure 3 for MON show the precipitation (P) and temperature (TM: mean temperature, TX: max temperature and TN: min temperature) time series of E-OBS, SPHERA, RCM and CPM for the period 2000-2018. In general, both RCM and CPM well reproduce SPHERA temporal variability, as also confirmed by the high and significant correlations for all the climate variables in both consortia (Table A 2). Nevertheless, both climate models tend to overestimate mean and maximum temperature while underestimating minimum temperature, as reflected by the statistical differences in mean values (Table A 3). Both climate models, and especially the RCM, underestimate precipitation in FRA, while the CPM tends to overestimate it in MON. Precipitation in MON is slightly overestimated also by the RCM. In FRA, RCM is closer to E-OBS mean values than CPM (Table A 3). However, in MON, E-OBS minimum temperature time series shows a strong decrease of almost 2°C between 2015 and 2018 (Figure 3), which is not observed in any models nor SPHERA. Further investigations revealed that this temperature decline is observed throughout the entire TOS and is inconsistent with other observational records (not shown). This E-OBS misrepresentation of the temperature field has a subsequent effect on the mean and minimum temperature time series (Figure 3), the temporal correlations (Table A 2), and is likely to be reflected in the temperature-based bioclimatic indices in TOS region, and at local scale in MON.

The time series of the bioclimatic indices considered are shown in Figure 4 and Figure 5. All the bioclimatic indices show very high and significant temporal correlation between SPHERA and both RCM and CPM in both consortia, as shown by Figure 6a and Figure 7a. The correlation are particularly high (i.e. above 0.8) for all temperature-based bioclimatic indices except for TnVeg and TxVeg, which appear more sensitive to the biases in minimum and maximum temperature (Figure 2 and Figure 3). The correlations with precipitation-based indices are still high (between 0.64 and 0.91) for SprR but drop for GSP in MON for both CPM and RCM. Similar conclusion can be drawn for the comparison of the climate models with E-OBS in FRA, while in MON four temperature-base indices (i.e. BEDD, WI, TnVeg, CNI) are not significantly correlated, likely due to the low correlations in medium and minimum temperature (Table A 2). The correlations, especially with SPHERA, tend to be slightly higher for the CPM than for the RCM for most indices, despite the higher NRMSE in the CPM (Figure 6b and Figure 7b). The

strong correlation between SPHERA and climate simulations (Figure 6a and Figure 7a) indicates that RCM and CPM reproduce the same temporal variability in the bioclimatic indices as SPHERA, despite the statistical differences in mean values (Table A 4). The same conclusion is valid also for the comparison of RCM and CPM to E-OBS at least for FRA. This analysis suggests both CPM and RCM could be a valid alternative to the reanalysis product to investigate the impact of climate on viticulture, despite the biases affecting the climate simulations. In addition, the reanalysis allows a more realistic representation of bioclimatic indices overcoming the pitfalls of the observational dataset E-OBS in TOS.

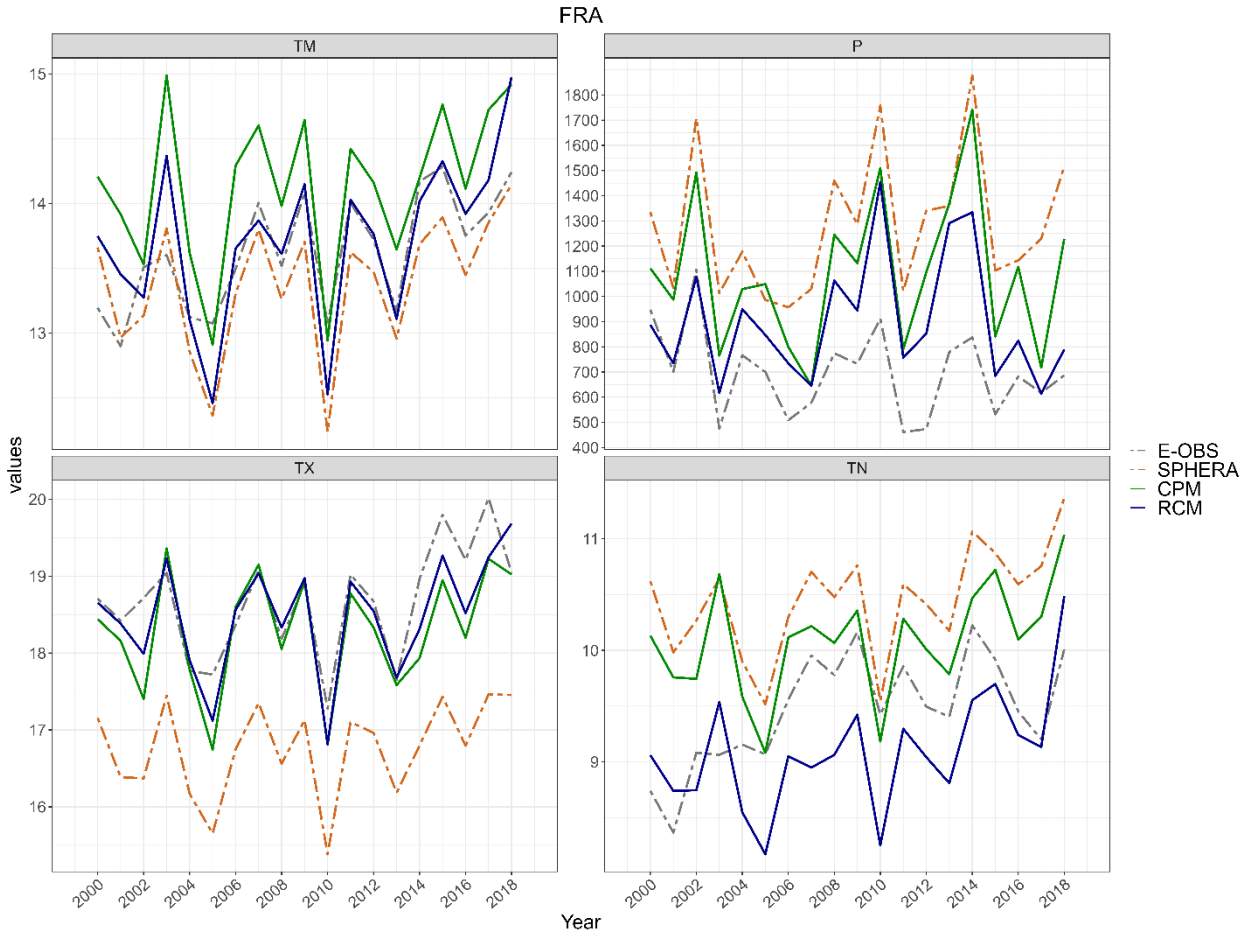

Figure 2: Time series of mean (TM), maximum Temperature (TX), minimum (TN) temperature and precipitation (P) over FRA area for E-OBS (dashed grey), SPHERA (dashed red), RCM (solid blue) and CPM (solid green) for the period 2000-2018. All the time series are based on data remapped on E-OBS grid (~ 11 km).

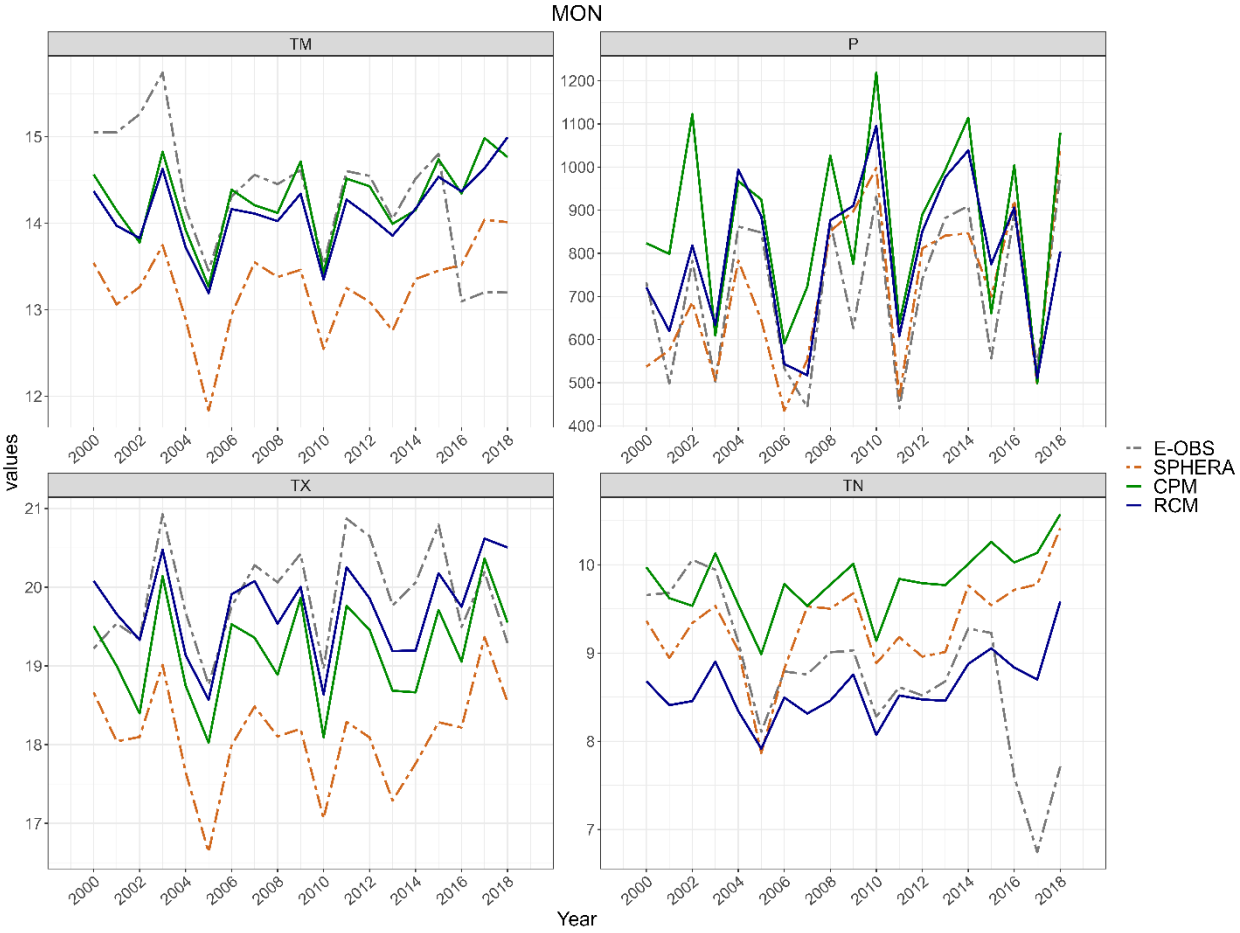

Figure 3: Time series of mean (TM), maximum Temperature (TX), minimum (TN) temperature and precipitation (P) over MON area for E-OBS (dashed grey), SPHERA (dashed red), RCM (solid blue) and CPM (solid green) for the period 2000-2018. All the time series are based on data remapped on E-OBS grid (~ 11 km).

Figure 4: Time series of the bioclimatic indices considered: Biologically Effective Degree Days (BEDD), Heliothermic Huglin index (HI), Winkler index (WI), Daily mean temperature during vegetation period (TmVeg), Minimum temperature during vegetative period (TnVeg), maximum temperature during vegetative period (TxVeg), Cool Night Index (CNI), Minimum temperature during rest period (TnRest), Growing season precipitation index (GSP) and Spring Rain index (SprR). over FRA area for E-OBS (dashed grey), SPHERA (dashed red), RCM (solid blue) and CPM (solid green) for the period 2000-2018. All the time series are based on data remapped on E-OBS grid (~ 11 km).

Figure 5: Time series of the bioclimatic indices considered: Biologically Effective Degree Days (BEDD), Heliothermic Huglin index (HI), Winkler index (WI), Daily mean temperature during vegetation period (TmVeg), Minimum temperature during vegetative period (TnVeg), maximum temperature during vegetative period (TxVeg), Cool Night Index (CNI), Minimum temperature during rest period (TnRest), Growing season precipitation index (GSP) and Spring Rain index (SprR). over MON area for E-OBS (dashed grey), SPHERA (dashed red), RCM (solid blue) and CPM (solid green) for the period 2000-2018. All the time series are based on data remapped on E-OBS grid (~ 11 km).

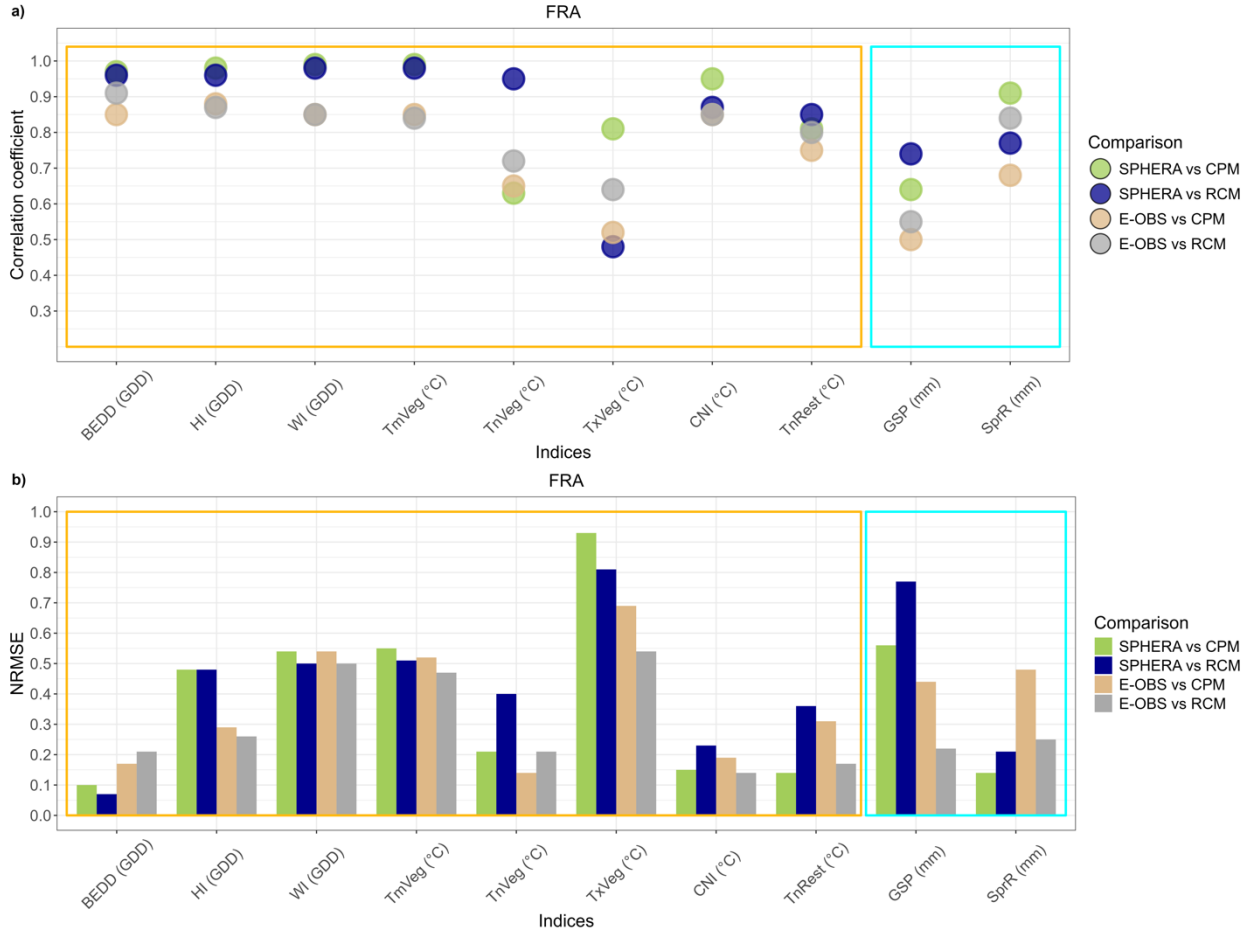

Figure 6: For the FRA area, the figure shows: in panel a, the Spearman correlation coefficient of the indices time series; in panel b, the Normalised Root Mean Square Error (NRMSE) with respect to the range of values (y_{max}-y_{min}) of the reference (SPHERA and E-OBS). Colours represent the different comparison performed and full coloured dots in panel a indicate a statistically significant result (p>=0.05)

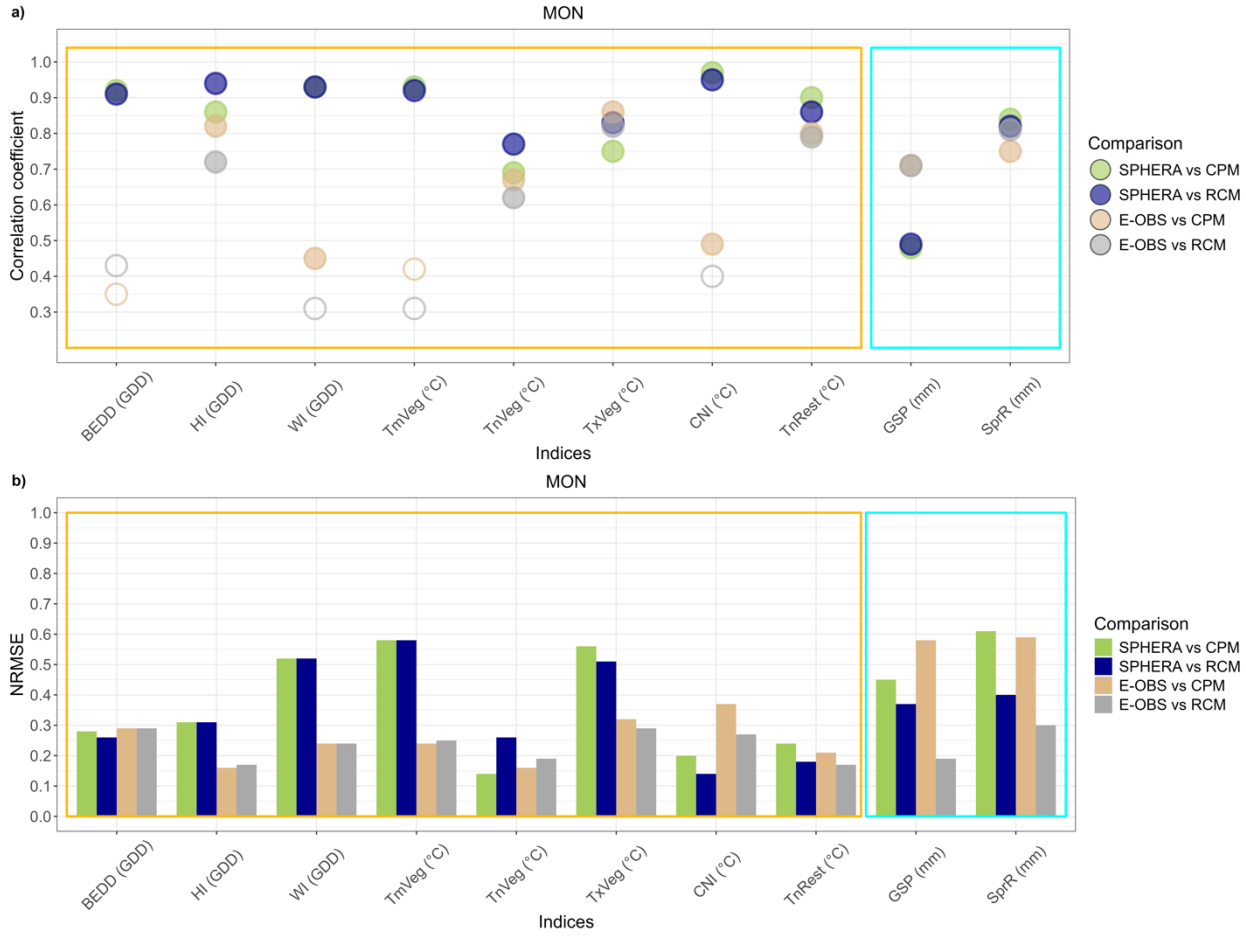

Figure 7: For the MON area, the figure shows: in panel a, the Spearman correlation coefficient of the indices time series; in panel b, the Normalised Root Mean Square Error (NRMSE) with respect to the range of values (y_{max}-y_{min}) of the reference (SPHERA and E-OBS). Colours represent the different comparison performed and full coloured dots in panel a indicate a statistically significant result (p>=0.05)

3.2 Bioclimatic indices control on wine grape productivity

3.2.1 Single regression analysis

A Spearman correlation analysis is performed to investigate the relation between the different bioclimatic indices and wine grape productivity and consequently determine the amount of total productivity variability (interannual and long-term) explained by these indices.

In FRA, the correlation coefficients are similar between climate simulations, observations, and reanalysis for some of the temperature-based indices, while diverge and are not significant for the precipitation-based ones (Figure 8). Statistically significant cases are: CNI with climate model simulations, SPHERA, and E-OBS; the BEDD index only when RCM and E-

OBS are used. Nevertheless, some of these bioclimatic indices (i.e. BEDD for E-OBS and CNI for CPM) as well as the FRA productivity show significant trends (Table A 5 and Table A 7), thus these significant correlations may depend on the long-term variability (i.e. the trend) rather than on the interannual variability. The RCM presents a statistically significant and positive correlation also between productivity and TnRest, which does not show trend over the period 2000-2018, suggesting that TnRest variability has a role in controlling productivity at the interannual time scale. The statistically significant coefficients are all positive indicating a positive effect on productivity of BEDD, CNI and TnRest.

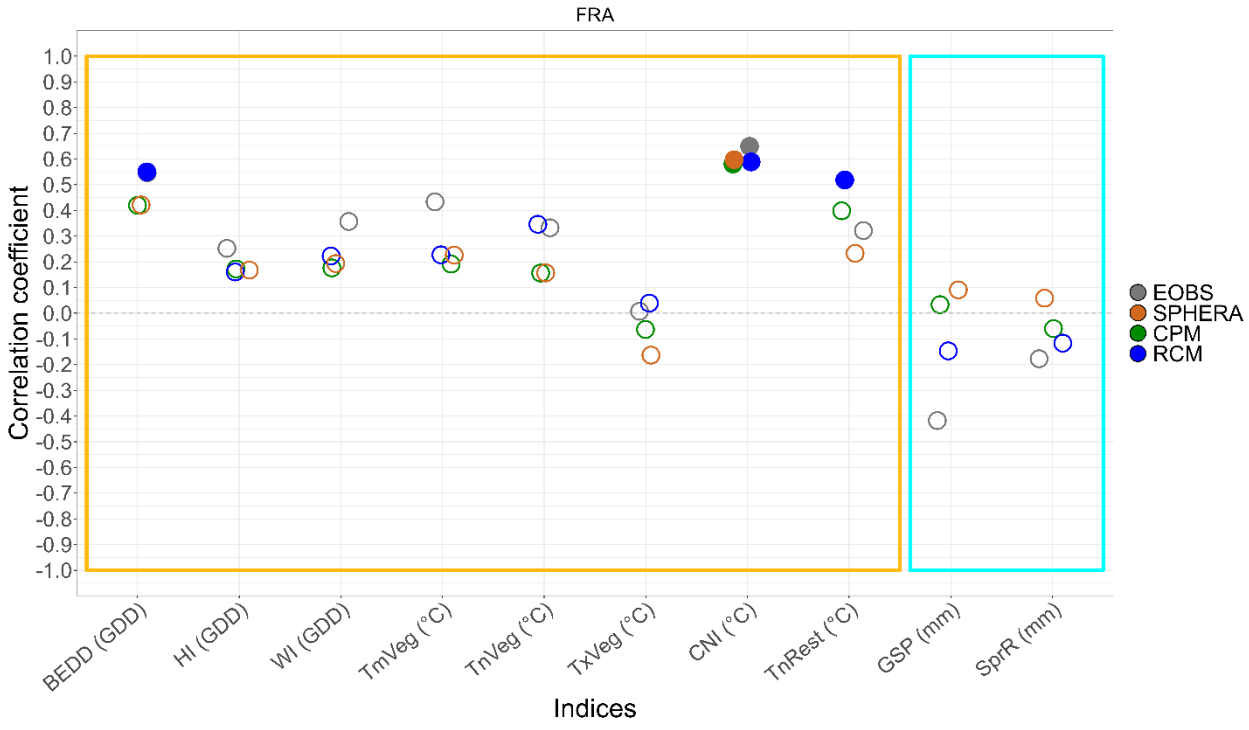

Figure 8: Spearman correlations coefficients between bioclimatic indices and wine grape productivity in FRA. Full coloured circles indicate significant correlations (p<=0.05).

In MON, the correlations between productivity and bioclimatic indices are similar across all the datasets for BEDD, HI, WI and TmVeg but show greater variation for all other temperature-based and precipitation-based indices (Figure 9). Significant results are found for TnVeg, only using CPM, and for TxVeg in all datasets. It is notable that TxVeg displays a negative correlation, indicating that extreme temperatures during the growing period have a detrimental effect on production. This aligns with wine makers expectations and is partially supported by the results from FRA (Figure 8), despite not being statistically significant. Both TnVeg and TxVeg indices show a significant positive trend for most datasets (Table A 6), which suggests productivity being more sensitive to the long-term variability. Productivity data do not show any trend in MON (Table A 7).

Only the CPM simulation shows significant correlation for the precipitation-based index GSP. This could be linked to the more realistic representation of the precipitation field (Prein et al., 2015), although positive correlations with GSP are not expected, as an excessively wet season is usually detrimental to production. Thus, it is possible that other factors influence this correlation, such as specific viticultural practices or vintage management (Priori et al., 2019). For example, harvesting immediately after rainfall may result in the collection of larger grapes, thus increasing the productivity. Additionally, specific trimming techniques can improve the ventilation between the branches, reducing the risk of mould and fungus, and thus limiting the negative impact of precipitation on the harvest (Evers et al., 2010).

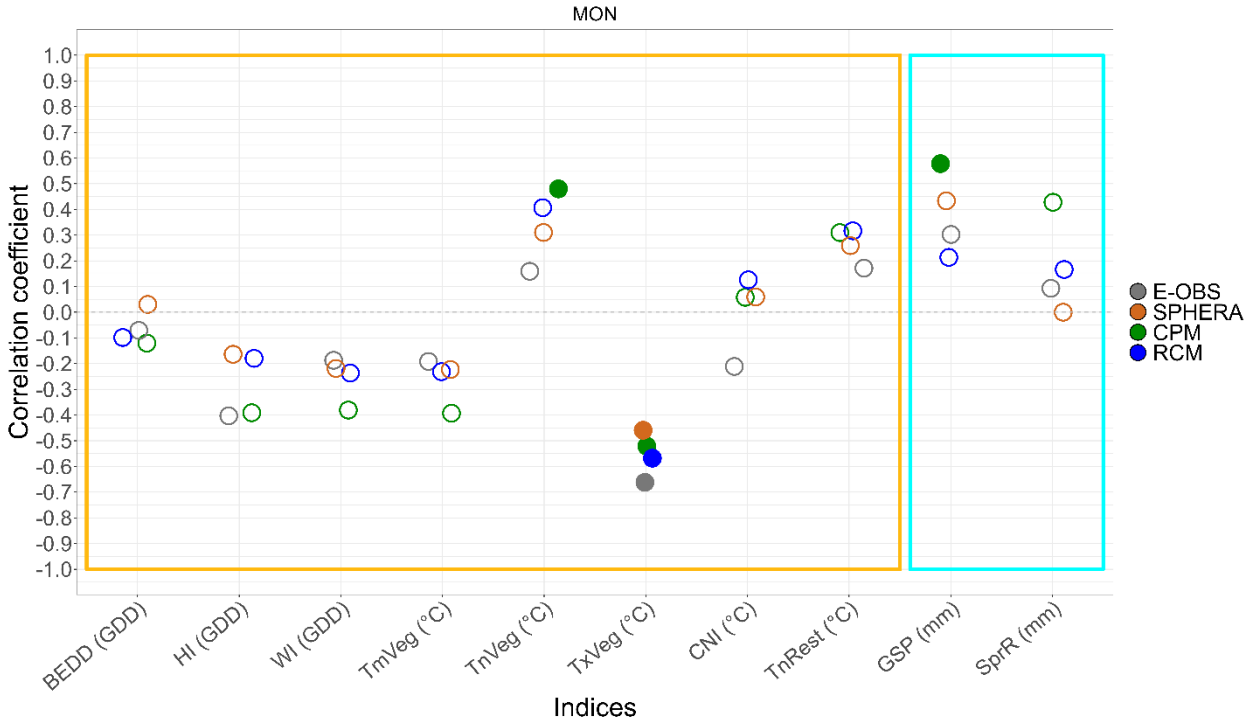

Figure 9: Spearman correlations between bioclimatic indices and wine grape productivity in MON. Full coloured circles indicate significant correlations (p<=0.05).

3.2.2 Multiple regression analysis

A multiple regression (MR) analysis is carried out and compared with the single regression (SR) approach to see if considering a linear combination of bioclimatic indices increases the proportion of productivity variability explained by the indices.

Table 2 shows the results of the MR model, highlighting the selected bioclimatic indices and the variance explained in comparison with the SR method, for each case in both FRA and MON. The authors highlight that, even when the MR selects just one index, this can differ from the single regression due to the correlation method chosen. The MR confirms that the temperature-based bioclimatic indices are more relevant than precipitation-based ones in explaining productivity variability, especially in FRA, where only for RCM the GSP is selected as a predictor. The selection of GSP for the RCM is unexpected.

Indeed, although GSP from the RCM shows high and significant correlations with both the CPM (not shown) and SPHERA (Figure 6), it is not selected by the MR model for the CPM and SPHERA. The comparison between the standardised beta coefficients (Dodge, 2008) of the MR model for RCM in FRA shows that GSP has the least impact on the explained variance of the observed productivity, suggesting that the selection of GSP for the RCM only might be an artifact of the statistical model. In MON, precipitation-based indices are selected as predictors in the MR model when using the CPM simulation and SPHERA reanalysis, confirming the relative higher importance of precipitation on productivity in this area compared to FRA. Thus, for MON, the improved representation of the precipitation field at convection-permitting scale could be a relevant factor, since in other datasets at coarser resolution (i.e. E-OBS and RCM) precipitation-based indices are excluded by the MR.

Table 2: Donuts chart indicating, for E-OBS, SPHERA, CPM and RCM, the best-performing index for the single regression (SR) and the indices included in the multiple regression model (MR), as well as the percentage of variance explained by each statistical model (centre of the donut), in FRA and MON. The percentage of variance is calculated as the squared coefficient of determination: of the Spearman correlation between the observed yield and best-performing bio-climatic index for SR; and of the Pearson correlation between the observed yield and the yield predicted using the MR model. Orange (blue) colour indicates temperature-based (precipitation-based) indices. The MR Adjusted R2 is expressed in the MR Adj R^2 column.

	FRA		MON	
Data	SR	MR	SR	MR
E-OBS	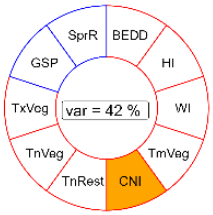	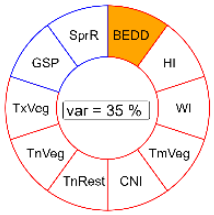	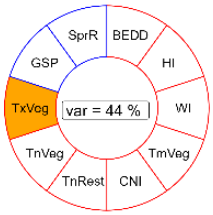	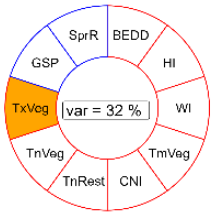
		MR $AdjR^2$ = 0.31		MR $AdjR^2$ = 0.28
SPHERA	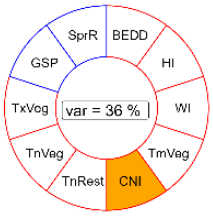	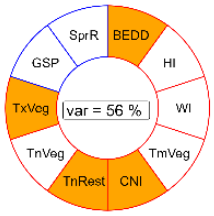	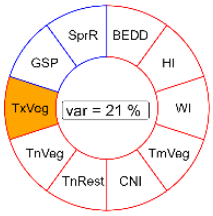	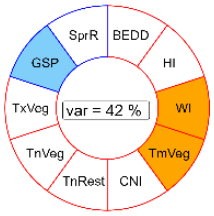
		MR $AdjR^2$ = 0.43		MR $AdjR^2$ = 0.31
CPM	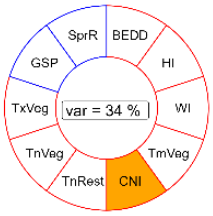	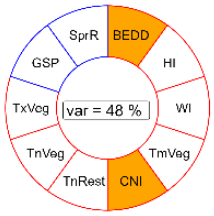	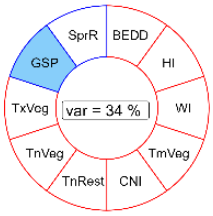	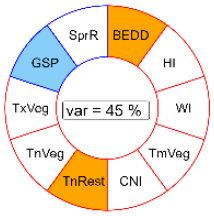

	MR AdjR^2 = 0.42	MR AdjR^2 = 0.34
RCM	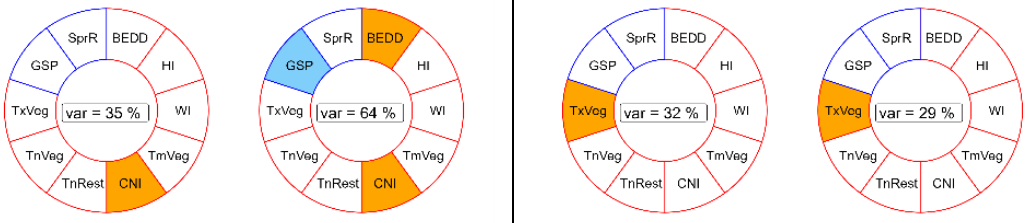	
	MR AdjR^2 = 0.57	MR AdjR^2 = 0.25

The overview on the performance of the single-regression method (SR) and the multiple regression method (MR) is presented in Figure 10, showing that using a linear combination of bioclimatic indices increases the proportion of explained total productivity variability, especially for FRA.

Overall, the bioclimatic indices explain a higher proportion of productivity variance in FRA compared to MON (Figure 10a and Table A 8), in line with previous findings at regional level for LOM and TOS (Massano et al., 2023). The highest proportion of explained variance in productivity is obtained in FRA with the MR approach and RCM data (64%), followed by SPHERA (56%) and CPM (48%). The variance explained in MON is lower, with a maximum of 45% obtained for CPM and the MR approach, very close to SPHERA with MR (42%) and to E-OBS with SR (44%).

The maximum variance in productivity explained by the SR is compared with the MR variance (Figure 10b). The comparison demonstrates that the MR better represents productivity variability in FRA in all cases except E-OBS, which shows a slight decrease in performance (-7%). Meanwhile, SPHERA gains 20%, the CPM 14% and the RCM 29% when MR is compared to SR. In MON, MR provides a better explanation for productivity variance in SPHERA reanalysis and CPM simulation, accounting for an increase of 11% and 21% respectively. However, for the E-OBS dataset and RCM simulation, MR performance decreases slightly (-12% and -3% respectively). To note that the decrease in performance from SR to MR method only occurs when only one bioclimatic index is selected in the MR. This could be linked to coefficient included in the MR (i.e. productivity=a_1*Index$_1$) or to the different type of correlation used in SR (Spearman) and MR (Pearson).

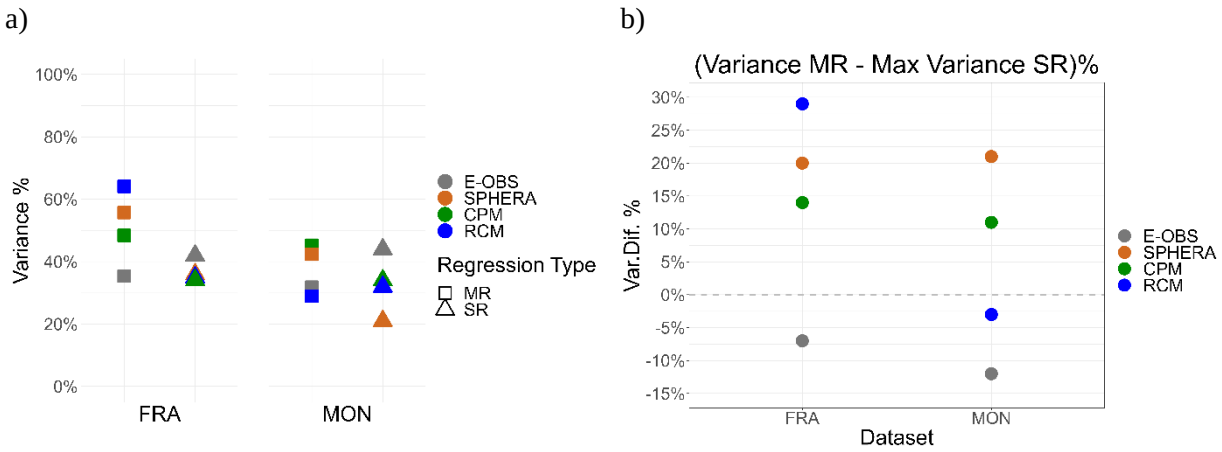

Figure 10: a) The maximum fraction of the wine grape productivity variance (%) explained by SR and MR in each consortium, colours indicate the type of climatic data used, squared (triangular) shape indicates multi regressive (single regressive) approach. b) Variance differences in percentage between MR and SR for FRA and MON.

4 Discussion and conclusion

This study represents, to the best of the authors' knowledge, the first application of a CPM to investigate the impact of climate variability and change on wine grape productivity, through the use of bioclimatic indices. The CPM simulation is compared with an RCM simulation, SPHERA reanalysis, and E-OBS observations for the period 2000-2018. The study presented here focuses on the local scale using wine grape productivity data from two Italian wine consortia, namely 'Consorzio per la tutela del Franciacorta' (FRA) and 'Consorzio Del Vino Nobile di Montepulciano' (MON). A multiple regression approach is used, in addition to a single regression method, to account for the possible interplay of bioclimatic indices in explaining wine grape productivity variability.

Overall, the single regression exhibits high correlation coefficients, but statistically significant results are only found for a small number of indices at the 95% confidence level. When more than one bioclimatic index is relevant, the multiple regression method outperforms the single regression systematically enhancing the explanatory power of bioclimatic indices regarding productivity variability. Furthermore, the method has the potential to select the predictors that are fit for purpose.

In FRA, the correlation coefficients are exclusively positive, and statistically significant only for temperature-based indices such as BEDD, CNI, and TnRest. Correlations with precipitation-based indices in FRA are not significant and tend to show negative relationships with productivity. These findings suggest that temperature is the main factor affecting production, while precipitation has a negative impact on productivity, potentially resulting in losses due to fungal diseases in the region.

The MON results indicate that only the convection-permitting resolution of the CPM and SPHERA provides statistically significant results for a precipitation-based index (GSP), highlighting the importance of km-scale resolution when precipitation

is a dominant factor for productivity. Also, RCM and E-OBS in this region show positive correlations between precipitation-based indices and productivity, even if they are not significant. This differs from the findings for FRA, where the correlations are negative, even if not significant. However, it is worth noting that there are many differences in the geographical features and types of wine produced in FRA and MON. FRA is in the humid subtropical climatic zone, while MON is situated in the hot summer Mediterranean zone. Other factors, such as vintage management techniques and cultivar selection, can also influence the productivity variability in addition to climate, but the investigation of these factors is beyond the scope of this paper. Meanwhile, the productivity for both FRA and MON exhibits a negative correlation with TxVeg with all the climatic data considered, but it is only significant for MON. This suggests that extreme maximum temperatures during the vegetative season (1st April - 30th October) may have harmful effects.

These results, which are obtained at the local scale using data from wine consortia, complement and expand the previous study conducted at the regional scale by Massano et al. (2023) using ISTAT productivity data and E-OBS (v26, resolution ~11 km) climate data. In fact, they did not find any statistically significant correlations for LOM or TOS region, where FRA and MON respectively lie, neither with temperature-based nor precipitation-based indices. At the contrary, in this work the MR can explain up to 64% in FRA with RCM and 45% in MON with the CPM. This indicates that working at a local scale and including a larger variety of bioclimatic indices is crucial to improve the portion of productivity variance explained by the bioclimatic indices.

The reanalysis dataset SPHERA outperforms the observational dataset E-OBS, in both MON and FRA with the MR approach, confirming to be a valuable alternative to observations. When the MR approach is applied, climate models appear to be a useful tool to explain the variability of productivity, improving the results obtained using E-OBS. However, the use of the CPM does not show a clear added value with respect to the RCM, since it performs better in MON, but not in FRA. This could be linked to the fact that temperature is generally the main driver of wine grape production, and the added value of the CPM become more evident when precipitation is a dominant factor, as in MON. Nevertheless, in a changing climate, with precipitation frequency and intensity expected to change (Tramblay and Somot, 2018; Zittis et al., 2021), the relevance of precipitation, along with precipitation-based bioclimatic indices, for grape productivity might increase and in turn the use of CPM might become crucial. The analysis presented here pave the path to the use of climate models to investigate the impact of climate change on wine production in the future. In this context, CPMs can provide new climate information, such as hail risk, which is a convections-related phenomenon that impact grape productivity. Moreover, this work shows an application of the bioclimatic indices to wine grape productivity that is rarely used.

Data availability

Data can be provided by the corresponding authors upon request.

Author contribution

LM, GF and MG conceived the study and conceptualised the methodology and the paper. LM collected the data, performed the analysis and wrote the paper. CC performed the climate model simulations. All the authors reviewed and edited the paper.

Competing interests

The authors declare that they have no conflict of interest.

Acknowledgments

The work presented in this paper has been developed within the framework of the project "Dipartimento di Eccellenza 2023-2027", funded by the Italian Ministry of Education, University and Research at IUSS Pavia.

The authors gratefully acknowledge the WCRP-CORDEX-FPS on Convective phenomena at high resolution over Europe and the Mediterranean [FPSCONV-ALP-3]. This work is part of the Med-CORDEX initiative (http://www.medcordex.eu).

The authors want to express sincere gratitude to the 'Consorzio per la tutela del Franciacorta' and the 'Consorzio Del Vino Nobile di Montepulciano' for the invaluable contribution provided in supplying the necessary data for this study.

References

Adão, F., Campos, J. C., Santos, J. A., Malheiro, A. C., and Fraga, H.: Relocation of bioclimatic suitability of Portuguese grapevine varieties under climate change scenarios, Front Plant Sci, 14, https://doi.org/10.3389/fpls.2023.974020, 2023.

Agnoli, L., Charters, S., Marks, D., and Tavilla, V.: Old world assessment of new world provenance cues: An Italian perspective, International Journal of Market Research, 65, 708–725, https://doi.org/10.1177/14707853231202759, 2023.

Agyeman, R. Y. K., Huo, F., Li, Z., Li, Y., Elshamy, M. E., and Hwang, Y.: Impact of climate change under the RCP8.5 emission scenario on multivariable agroclimatic indices in Western Canada from convection-permitting climate simulation, Anthropocene, 44, 100408, https://doi.org/10.1016/j.ancene.2023.100408, 2023.

Amerine, M. A. and Winkler, A. J.: Composition and quality of musts and wines of California grapes, A Journal of Agricultural Science Published by the California Agricultural Experiment Statio, 15, 493–673, 1944.

Anderson, J. D., Jones, G. V, Tait, A., Hall, A., and Trought, M. C. T.: Analysis of viticulture region climate structure and suitability in New Zealand, J. Int. Sci. Vigne Vin, 149–165 pp., 2012.

Aswad, F., Yousif, A., and Ibrahim, S.: Trend Analysis Using Mann-kendall And Sen's Slope Estimator Test for Annual And Monthly Rainfall for Sinjar District, Iraq, The Journal of the University of Duhok, 23, 501–508, https://doi.org/10.26682/csjuod.2020.23.2.41, 2020.

Badr, G., Hoogenboom, G., Abouali, M., Moyer, M., and Keller, M.: Analysis of several bioclimatic indices for viticultural zoning in the Pacific Northwest, Clim Res, 76, 203–223, https://doi.org/10.3354/cr01532, 2018.

Bagagiolo, G., Rabino, D., Biddoccu, M., Nigrelli, G., Berro, D. C., Mercalli, L., Spanna, F., Capello, G., and Cavallo, E.: Effects of inter-annual climate variability on grape harvest timing in rainfed hilly vineyards of piedmont (NW Italy), Italian Journal of Agrometeorology, 2021, 37–49, https://doi.org/10.36253/ijam-1083, 2021.

Baldauf, M., Seifert, A., Förstner, J., Majewski, D., Raschendorfer, M., and Reinhardt, T.: Operational Convective-Scale Numerical Weather Prediction with the COSMO Model: Description and Sensitivities, Mon Weather Rev, 139, 3887–3905, https://doi.org/10.1175/MWR-D-10-05013.1, 2011.

Bamba, A., Kouadio, K., Toure, D. E., Jackson, L., Marsham, J., Roberts, A., and Yoshioka, M.: Simulating the impact of varying vegetation on West African monsoon surface fluxes using a regional convection-permitting model, Plant-Environment Interactions, 4, 134–145, https://doi.org/10.1002/pei3.10107, 2023.

Ban, N., Caillaud, C., Coppola, E., Pichelli, E., Sobolowski, S., Adinolfi, M., Ahrens, B., Alias, A., Anders, I., Bastin, S., Belušić, D., Berthou, S., Brisson, E., Cardoso, R. M., Chan, S. C., Christensen, O. B., Fernández, J., Fita, L., Frisius, T., Gašparac, G., Giorgi, F., Goergen, K., Haugen, J. E., Hodnebrog, Ø., Kartsios, S., Katragkou, E., Kendon, E. J., Keuler, K., Lavin-Gullon, A., Lenderink, G., Leutwyler, D., Lorenz, T., Maraun, D., Mercogliano, P., Milovac, J., Panitz, H. J., Raffa, M., Remedio, A. R., Schär, C., Soares, P. M. M., Srnec, L., Steensen, B. M., Stocchi, P., Tölle, M. H., Truhetz, H., Vergara-Temprado, J., de Vries, H., Warrach-Sagi, K., Wulfmeyer, V., and Zander, M. J.: The first multi-model ensemble of regional climate simulations at kilometer-scale resolution, part I: evaluation of precipitation, Clim Dyn, 57, 275–302, https://doi.org/10.1007/s00382-021-05708-w, 2021.

Berg, P., Wagner, S., Kunstmann, H., and Schädler, G.: High resolution regional climate model simulations for Germany: part I—validation, Clim Dyn, 40, 401–414, https://doi.org/10.1007/s00382-012-1508-8, 2013.

Bernetti, I., Menghini, S., Marinelli, N., Sacchelli, S., and Sottini, V. A.: Assessment of climate change impact on viticulture: Economic evaluations and adaptation strategies analysis for the Tuscan wine sector, Wine Economics and Policy, 1, 73–86, https://doi.org/10.1016/j.wep.2012.11.002, 2012.

Berthou, S., Kendon, E. J., Rowell, D. P., Roberts, M. J., Tucker, S., and Stratton, R. A.: Larger Future Intensification of Rainfall in the West African Sahel in a Convection-Permitting Model, Geophys Res Lett, 46, 13299–13307, https://doi.org/10.1029/2019GL083544, 2019.

Blanco-Ward, D., García Queijeiro, J. M., and Jones, G. V.: Spatial climate variability and viticulture in the Miño River Valley of Spain, Vitis - Journal of Grapevine Research, 46, 63–70, 2007.

Brisson, E., Van Weverberg, K., Demuzere, M., Devis, A., Saeed, S., Stengel, M., and van Lipzig, N. P. M.: How well can a convection-permitting climate model reproduce decadal statistics of precipitation, temperature and cloud characteristics?, Clim Dyn, 47, 3043–3061, https://doi.org/10.1007/s00382-016-3012-z, 2016.

Cabré, F. and Nuñez, M.: Impacts of climate change on viticulture in Argentina, Reg Environ Change, 20, https://doi.org/10.1007/s10113-020-01607-8, 2020.

Caillaud, C., Somot, S., Alias, A., Bernard-Bouissières, I., Fumière, Q., Laurantin, O., Seity, Y., and Ducrocq, V.: Modelling Mediterranean heavy precipitation events at climate scale: an object-oriented evaluation of the CNRM-AROME convection-permitting regional climate model, Clim Dyn, 56, 1717–1752, https://doi.org/10.1007/S00382-020-05558-Y, 2021.

Cerenzia, I. M. L., Giordani, A., Paccagnella, T., and Montani, A.: Towards a convection-permitting regional reanalysis over the Italian domain, Meteorological Applications, 29, https://doi.org/10.1002/met.2092, 2022.

Chapman, S., E Birch, C., Pope, E., Sallu, S., Bradshaw, C., Davie, J., and H Marsham, J.: Impact of climate change on crop suitability in sub-Saharan Africa in parameterized and convection-permitting regional climate models, Environmental Research Letters, 15, https://doi.org/10.1088/1748-9326/ab9daf, 2020.

Chapman, S., Bacon, J., Birch, C. E., Pope, E., Marsham, J. H., Msemo, H., Nkonde, E., Sinachikupo, K., and Vanya, C.: Climate Change Impacts on Extreme Rainfall in Eastern Africa in a Convection-Permitting Climate Model, J Clim, 36, 93–109, https://doi.org/10.1175/JCLI-D-21-0851.1, 2023.

Chou, C., Marcos-Matamoros, R., Garcia, L. P., Pérez-Zanón, N., Teixeira, M., Silva, S., Fontes, N., Graça, A., Dell'Aquila, A., Calmanti, S., and González-Reviriego, N.: Advanced seasonal predictions for vine management based on bioclimatic indicators tailored to the wine sector, Clim Serv, 30, 100343, https://doi.org/10.1016/j.cliser.2023.100343, 2023.

Christensen, J. H., Boberg, F., Christensen, O. B., and Lucas-Picher, P.: On the need for bias correction of regional climate change projections of temperature and precipitation, Geophys Res Lett, 35, https://doi.org/10.1029/2008GL035694, 2008.

Coppola, E., Sobolowski, S., Pichelli, E., Raffaele, F., Ahrens, B., Anders, I., Ban, N., Bastin, S., Belda, M., Belusic, D., Caldas-Alvarez, A., Cardoso, R. M., Davolio, S., Dobler, A., Fernandez, J., Fita, L., Fumiere, Q., Giorgi, F., Goergen, K., Güttler, I., Halenka, T., Heinzeller, D., Hodnebrog, Jacob, D., Kartsios, S., Katragkou, E., Kendon, E., Khodayar, S., Kunstmann, H., Knist, S., Lavín-Gullón, A., Lind, P., Lorenz, T., Maraun, D., Marelle, L., van Meijgaard, E., Milovac, J., Myhre, G., Panitz, H. J., Piazza, M., Raffa, M., Raub, T., Rockel, B., Schär, C., Sieck, K., Soares, P. M. M., Somot, S., Srnec, L., Stocchi, P., Tölle, M. H., Truhetz, H., Vautard, R., de Vries, H., and Warrach-Sagi, K.: A first-of-its-kind multi-model convection permitting ensemble for investigating convective phenomena over Europe and the Mediterranean, Clim Dyn, 55, 3–34, https://doi.org/10.1007/s00382-018-4521-8, 2020.

Costantini, E. A. C., Fantappié, M., and L'Abate, G.: Climate and Pedoclimate of Italy, 19–37, https://doi.org/10.1007/978-94-007-5642-7_2, 2013.

Dalla Marta, A., Grifoni, D., Mancini, M., Storchi, P., Zipoli, G., and Orlandini, S.: Analysis of the relationships between climate variability and grapevine phenology in the Nobile di Montepulciano wine production area, Journal of Agricultural Science, 148, 657–666, https://doi.org/10.1017/S0021859610000432, 2010.

Daniel, M., Lemonsu, A., Déqué, M., Somot, S., Alias, A., and Masson, V.: Benefits of explicit urban parameterization in regional climate modeling to study climate and city interactions, Clim Dyn, 52, 2745–2764, https://doi.org/10.1007/S00382-018-4289-X/TABLES/8, 2019.

Dee, D. P., Uppala, S. M., Simmons, A. J., Berrisford, P., Poli, P., Kobayashi, S., Andrae, U., Balmaseda, M. A., Balsamo, G., Bauer, P., Bechtold, P., M Beljaars, A. C., van de Berg, L., Bidlot, J., Bormann, N., Delsol, C., Dragani, R., Fuentes, M., Geer,

A. J., Haimberger, L., Healy, S. B., Hersbach, H., Isaksen, L., Kållberg, P., Köhler, M., Matricardi, M., McNally, A. P., Monge-Sanz, B. M., Morcrette, J., Park, B., Peubey, C., de Rosnay, P., Tavolato, C., Thépaut, J., Vitart, F., Acm, B., de Berg, van L., J-j, M., B-k, P., and Rosnay, de P.: The ERA-Interim reanalysis: configuration and performance of the data assimilation system, Quarterly Journal of the Royal Meteorological Society Q. J. R. Meteorol. Soc, 137, 553–597, https://doi.org/10.1002/qj.828, 2011.

Dell'Aquila, A.: Monitoring climate related risk and opportunities for the wine sector: the MED-GOLD pilot service CONFER: Co-production of Climate Services for East Africa View project WineBioCode View project, https://doi.org/10.5281/zenodo.6357144, 2022.

Dodge, Y.: The Concise Encyclopedia of Statistics, Springer New York, New York, NY, https://doi.org/10.1007/978-0-387-32833-1, 2008.

Düring, H.: Potential frost resistance of grape: Kinetics of temperature-induced hardening ofRiesling and Silvaner buds, Vitis, 213–214 pp., 1997.

Eccel, E., Zollo, A. L., Mercogliano, P., and Zorer, R.: Simulations of quantitative shift in bio-climatic indices in the viticultural areas of Trentino (Italian Alps) by an open source R package, Comput Electron Agric, 127, 92–100, https://doi.org/10.1016/j.compag.2016.05.019, 2016.

Evers, D., Molitor, D., Rothmeier, M., Behr, M., Fischer, S., and Hoffmann, L.: Efficiency of different strategies for the control of grey mold on grapes including gibberellic acid (Gibb3), leaf removal and/or botrycide treatments, Journal International des Sciences de la Vigne et du Vin, 44, 151–159, https://doi.org/10.20870/OENO-ONE.2010.44.3.1469, 2010.

Fosser, G., Kendon, E. J., Stephenson, D., and Tucker, S.: Convection-Permitting Models Offer Promise of More Certain Extreme Rainfall Projections, Geophys Res Lett, 47, e2020GL088151, https://doi.org/10.1029/2020GL088151, 2020.

Fosser, G., Gaetani M., Kendon, E. J. , M. , Adinolfi, M. , Ban, N. , Belušić, D. , Caillaud, C. , Cardoso, R. M. , Coppola, E. , Demory, M.-E. , De Vries, H. , Dobler, A. , Feldmann, H. , Görgen, K. , Lenderink, G. , Pichelli, E. , Schär, C. , Soares, P. M. M. , Somot, S. , and Tölle, M. H.: Convection-permitting climate models offer more certain extreme rainfall projections, NPJ Clim Atmos Sci, https://doi.org/10.21203/rs.3.rs-3365617/v1, 2024.

Fraga, H., García de Cortázar Atauri, I., Malheiro, A. C., and Santos, J. A.: Modelling climate change impacts on viticultural yield, phenology and stress conditions in Europe, Glob Chang Biol, 22, 3774–3788, https://doi.org/10.1111/gcb.13382, 2016.

Fumière, Q., Déqué, M., Nuissier, O., Somot, S., Alias, A., Caillaud, C., Laurantin, O., and Seity, Y.: Extreme rainfall in Mediterranean France during the fall: added value of the CNRM-AROME Convection-Permitting Regional Climate Model, Clim Dyn, 55, 77–91, https://doi.org/10.1007/S00382-019-04898-8/FIGURES/9, 2020.

Gaitán, E. and Pino-Otín, M. R.: Using bioclimatic indicators to assess climate change impacts on the Spanish wine sector, https://doi.org/10.1016/j.atmosres.2023.106660, 1 May 2023.

Gentilucci, M.: Temperature variations in Central Italy (Marche region) and effects on wine grape production, Theoretical and Applied Climatology, 140, 303–312, 2020.

Giordani, A., Cerenzia, I. M. L., Paccagnella, T., and Di Sabatino, S.: SPHERA, a new convection-permitting regional reanalysis over Italy: Improving the description of heavy rainfall, Quarterly Journal of the Royal Meteorological Society, 149, 781–808, https://doi.org/10.1002/qj.4428, 2023.

Giorgi, F.: Climate change hot-spots, Geophys Res Lett, 33, 1–4, https://doi.org/10.1029/2006GL025734, 2006.

Gladstones, J. S.: Viticulture and environment : a study of the effects of environment on grapegrowing and wine qualities, with emphasis on present and future areas for growing winegrapes in Australia, Winetitles, 1992.

Gori, C. and Alampi Sottini, V.: The role of the Consortia in the Italian wine production system and the impact of EU and national legislation, Wine Economics and Policy, 3, 62–67, https://doi.org/10.1016/j.wep.2014.05.001, 2014.

Hanif, M. F., Mustafa, M. R. U., Liaqat, M. U., Hashim, A. M., and Yusof, K. W.: Evaluation of Long-Term Trends of Rainfall in Perak, Malaysia, Climate, 10, https://doi.org/10.3390/cli10030044, 2022.

Hersbach, H., Bell, B., Berrisford, P., Hirahara, S., Horányi, A., Muñoz-Sabater, J., Nicolas, J., Peubey, C., Radu, R., Schepers, D., Simmons, A., Soci, C., Abdalla, S., Abellan, X., Balsamo, G., Bechtold, P., Biavati, G., Bidlot, J., Bonavita, M., De Chiara, G., Dahlgren, P., Dee, D., Diamantakis, M., Dragani, R., Flemming, J., Forbes, R., Fuentes, M., Geer, A., Haimberger, L., Healy, S., Hogan, R. J., Hólm, E., Janisková, M., Keeley, S., Laloyaux, P., Lopez, P., Lupu, C., Radnoti, G., de Rosnay, P., Rozum, I., Vamborg, F., Villaume, S., and Thépaut, J. N.: The ERA5 global reanalysis, Quarterly Journal of the Royal Meteorological Society, 146, 1999–2049, https://doi.org/10.1002/qj.3803, 2020.

Huglin M: Nouveau mode d'évaluation des possibilités héliothermiques d'un milieu viticole, Comptes Rendus de l'Académie d'Agriculture de France, 64, 1117–1126, 1978.

Hunter, J. J. and Bonnardot, V.: Suitability of some climatic parameters for grapevine cultivation in South Africa, with focus on key physiological processes, South African Journal of Enology and Viticulture, 32, 137–154, https://doi.org/10.21548/32-1-1374, 2011.

Jaeger, E. B. and Seneviratne, S. I.: Impact of soil moisture-atmosphere coupling on European climate extremes and trends in a regional climate model, Clim Dyn, 36, 1919–1939, https://doi.org/10.1007/S00382-010-0780-8/FIGURES/13, 2011.

James G, Witten D, Hastie T, and Tibshirani R: An Introduction to Statistical Learning: With Applications in R, 1st ed., Springer, 2013.

James, G., Witten, D., Hastie, T., and Tibshirani, R.: An Introduction to Statistical Learning with Applications in R Second Edition, Springer, 197–206 pp., 2021.

Jones, G. V., White, M. A., Cooper, O. R., and Storchmann, K.: Climate Change and Global Wine Quality, Clim Change, 73, 319–343, https://doi.org/10.1007/s10584-005-4704-2, 2005.

Kassambara, A.: Machine learning essentials, Practical Guide in R, 1st ed., CreateSpace Independent Publishing Platform, 77–82 pp., 2018.

Kendon, E. J., Ban, N., Roberts, N. M., Fowler, H. J., Roberts, M. J., Chan, S. C., Evans, J. P., Fosser, G., and Wilkinson, J. M.: Do convection-permitting regional climate models improve projections of future precipitation change?, Bull Am Meteorol Soc, 98, 79–93, https://doi.org/10.1175/BAMS-D-15-0004.1, 2017.

Koufos, G., Mavromatis, T., Koundouras, S., Fyllas, N. M., and Jones, G. V.: Viticulture-climate relationships in Greece: the impacts of recent climate trends on harvest date variation, International Journal of Climatology, 34, 1445–1459, https://doi.org/10.1002/joc.3775, 2014.

Kuhn, M. and Johnson, K.: Applied Predictive Modeling, Springer, 61–90 pp., 2013.

Kyselý, J. and Plavcová, E.: A critical remark on the applicability of E-OBS European gridded temperature data set for validating control climate simulations, Journal of Geophysical Research Atmospheres, 115, https://doi.org/10.1029/2010JD014123, 2010.

Lamichhane, J. R.: Rising risks of late-spring frosts in a changing climate, Nat Clim Chang, 11, 554–555, https://doi.org/10.1038/s41558-021-01090-x, 2021.

Leoni, B., Spreafico, M., Patelli, M., Soler, V., Garibaldi, L., and Nava, V.: Long-term studies for evaluating the impacts of natural and anthropic stressors on limnological features and the ecosystem quality of Lake Iseo, Adv Oceanogr Limnol, 10, https://doi.org/10.4081/aiol.2019.8622, 2019.

Liakopoulou, K. S. and Mavromatis, T.: Evaluation of Gridded Meteorological Data for Crop Sensitivity Assessment to Temperature Changes: An Application with CERES-Wheat in the Mediterranean Basin, Climate, 11, https://doi.org/10.3390/cli11090180, 2023.

Lisek, J.: Winter frost injury of buds on one-year-old grapevine shoots of Vitis vinifera cultivars and interspecific hybrids in Poland , Folia Horticulturae, 24, 97–103, https://doi.org/10.2478/V10245-012-0010-4, 2012.

Lorenz, P. and Jacob, D.: Validation of temperature trends in the ENSEMBLES regional climate model runs driven by ERA40, Clim Res, 44, 167–177, https://doi.org/10.3354/CR00973, 2010.

Lucas-Picher, P., Brisson, E., Caillaud, C., Alias, A., Nabat, P., Lemonsu, A., Poncet, N., Cortés Hernandez, V. E., Michau, Y., Doury, A., Monteiro, D., and Somot, S.: Evaluation of the convection-permitting regional climate model CNRM-AROME41t1 over Northwestern Europe, Clim Dyn, https://doi.org/10.1007/s00382-022-06637-y, 2023.

Malheiro, A. C., Campos, R., Fraga, H., Eiras-Dias, J., Silvestre, J., and Santos, J. A.: Winegrape phenology and temperature relationships in the Lisbon wine region, Portugal, Journal International des Sciences de la Vigne et du Vin, 47, 287–299, https://doi.org/10.20870/oeno-one.2013.47.4.1558, 2013.

Mann, H. B.: Nonparametric Tests Against Trend, Econometrica, 13, 245, https://doi.org/10.2307/1907187, 1945.

Massano, L., Fosser, G., Gaetani, M., and Bois, B.: Assessment of climate impact on grape productivity: A new application for bioclimatic indices in Italy, Science of the Total Environment, 905, https://doi.org/10.1016/j.scitotenv.2023.167134, 2023.

Nabat, P., Somot, S., Cassou, C., Mallet, M., Michou, M., Bouniol, D., Decharme, B., Drugé, T., Roehrig, R., and Saint-Martin, D.: Modulation of radiative aerosols effects by atmospheric circulation over the Euro-Mediterranean region, Atmos Chem Phys, 20, 8315–8349, https://doi.org/10.5194/ACP-20-8315-2020, 2020.

OIV: OIV Guidelines for studying climate variability on vitiviniculture in the context of climate change and its evelution, 1–7, 2015.

OIV: State of the world vitivinicultural sector in 2022, 2023.

Photiadou, C., Fontes, N., Rocha Graça, A., and Schrier, G. van der: ECA&D and E-OBS: High-resolution datasets for monitoring climate change and effects on viticulture in Europe, BIO Web Conf, 9, 01002, https://doi.org/10.1051/bioconf/20170901002, 2017.

Pichelli, E., Coppola, E., Sobolowski, S., Ban, N., Giorgi, F., Stocchi, P., Alias, A., Belušić, D., Berthou, S., Caillaud, C., Cardoso, R. M., Chan, S., Christensen, O. B., Dobler, A., de Vries, H., Goergen, K., Kendon, E. J., Keuler, K., Lenderink, G., Lorenz, T., Mishra, A. N., Panitz, H. J., Schär, C., Soares, P. M. M., Truhetz, H., and Vergara-Temprado, J.: The first multi-model ensemble of regional climate simulations at kilometer-scale resolution part 2: historical and future simulations of precipitation, Clim Dyn, 56, 3581–3602, https://doi.org/10.1007/S00382-021-05657-4, 2021.

Piña-Rey, A., González-Fernández, E., Fernández-González, M., Lorenzo, M. N., and Rodríguez-Rajo, Fco. J.: Climate Change Impacts Assessment on Wine-Growing Bioclimatic Transition Areas, Agriculture, 10, 605, https://doi.org/10.3390/agriculture10120605, 2020.

Prein, A. F., Langhans, W., Fosser, G., Ferrone, A., Ban, N., Goergen, K., Keller, M., Tölle, M., Gutjahr, O., Feser, F., Brisson, E., Kollet, S., Schmidli, J., Van Lipzig, N. P. M., and Leung, R.: A review on regional convection-permitting climate modeling: Demonstrations, prospects, and challenges, Reviews of Geophysics, 53, 323–361, https://doi.org/10.1002/2014RG000475, 2015.

Priori, S., Pellegrini, S., Perria, R., Puccioni, S., Storchi, P., Valboa, G., and Costantini, E. A. C.: Scale effect of terroir under three contrasting vintages in the Chianti Classico area (Tuscany, Italy), Geoderma, 334, 99–112, https://doi.org/10.1016/j.geoderma.2018.07.048, 2019.

Rafique, R., Ahmad, T., Kalsoom, T., Khan, M. A., and Ahmed, M.: Climatic Challenge for Global Viticulture and Adaptation Strategies, in: Global Agricultural Production: Resilience to Climate Change, Springer International Publishing, 611–634, https://doi.org/10.1007/978-3-031-14973-3_22, 2023.

Raül Marcos-Matamoros, Nube González-Reviriego, Antonio Graça, Alessandro Del Aquilla, Ilaria Vigo, S. S., Konstantinos V.Varotsos, and Michael Sanderson: Deliverable 3.2: Report on the methodology followed to implement the wine pilot services, 2020.

Retalis, A., Katsanos, D., and Michaelides, S.: Precipitation climatology over the Mediterranean Basin — Validation over Cyprus, Atmos Res, 169, 449–458, https://doi.org/10.1016/J.ATMOSRES.2015.01.012, 2016.

Roehrdanz, P. R. and Hannah, L.: Climate Change, California Wine, and Wildlife Habitat, Journal of Wine Economics, 11, 69–87, https://doi.org/10.1017/jwe.2014.31, 2016.

Le Roy, B., Lemonsu, A., and Schoetter, R.: A statistical–dynamical downscaling methodology for the urban heat island applied to the EURO-CORDEX ensemble, Clim Dyn, 56, 2487–2508, https://doi.org/10.1007/s00382-020-05600-z, 2021.

Ruti, P. M., Somot, S., Giorgi, F., Dubois, C., Flaounas, E., Obermann, A., Dell'Aquila, A., Pisacane, G., Harzallah, A., Lombardi, E., Ahrens, B., Akhtar, N., Alias, A., Arsouze, T., Aznar, R., Bastin, S., Bartholy, J., Béranger, K., Beuvier, J., Bouffies-Cloché, S., Brauch, J., Cabos, W., Calmanti, S., Calvet, J.-C., Carillo, A., Conte, D., Coppola, E., Djurdjevic, V., Drobinski, P., Elizalde-Arellano, A., Gaertner, M., Galàn, P., Gallardo, C., Gualdi, S., Goncalves, M., Jorba, O., Jordà, G.,

L'Heveder, B., Lebeaupin-Brossier, C., Li, L., Liguori, G., Lionello, P., Maciàs, D., Nabat, P., Önol, B., Raikovic, B., Ramage, K., Sevault, F., Sannino, G., Struglia, M. V., Sanna, A., Torma, C., and Vervatis, V.: Med-CORDEX Initiative for Mediterranean Climate Studies, Bull Am Meteorol Soc, 97, 1187–1208, https://doi.org/10.1175/BAMS-D-14-00176.1, 2016.

Sacchelli, S., Fabbrizzi, S., Bertocci, M., Marone, E., Menghini, S., and Bernetti, I.: A mix-method model for adaptation to climate change in the agricultural sector: A case study for Italian wine farms, J Clean Prod, 166, 891–900, https://doi.org/10.1016/j.jclepro.2017.08.095, 2017.

Sánchez, Y., Martínez-Graña, A. M., Santos-Francés, F., and Yenes, M.: Index for the calculation of future wine areas according to climate change application to the protected designation of origin "Sierra de Salamanca" (Spain), Ecol Indic, 107, https://doi.org/10.1016/j.ecolind.2019.105646, 2019.

Santillán, D., Garrote, L., Iglesias, A., and Sotes, V.: Climate change risks and adaptation: new indicators for Mediterranean viticulture, Mitig Adapt Strateg Glob Chang, 25, 881–899, https://doi.org/10.1007/s11027-019-09899-w, 2020.

Schättler, U., Doms, G., and Schraff, C.: A Description of the Nonhydrostatic Regional COSMO-Model - Part VII: User's Guide., 195 pp., 2018.

Van Der Schrier, G., Van Den Besselaar, E. J. M., Klein Tank, A. M. G., and Verver, G.: Monitoring European average temperature based on the E-OBS gridded data set, Journal of Geophysical Research Atmospheres, 118, 5120–5135, https://doi.org/10.1002/jgrd.50444, 2013.

Sgubin, G., Swingedouw, D., Dayon, G., García de Cortázar-Atauri, I., Ollat, N., Pagé, C., and van Leeuwen, C.: The risk of tardive frost damage in French vineyards in a changing climate, Agric For Meteorol, 250–251, 226–242, https://doi.org/10.1016/j.agrformet.2017.12.253, 2018.

Sgubin, G., Swingedouw, D., Mignot, J., Gambetta, G. A., Bois, B., Loukos, H., Noël, T., Pieri, P., García de Cortázar-Atauri, I., Ollat, N., and van Leeuwen, C.: Non-linear loss of suitable wine regions over Europe in response to increasing global warming, Glob Chang Biol, 29, 808–826, https://doi.org/10.1111/gcb.16493, 2023.

Spielmann, N. and Charters, S.: The dimensions of authenticity in terroir products, International Journal of Wine Business Research, 25, 310–324, https://doi.org/10.1108/IJWBR-01-2013-0004, 2013.

Stauffer, D. R. and Seaman, N. L.: Use of Four-Dimensional Data Assimilation in a Limited-Area Mesoscale Model. Part I: Experiments with Synoptic-Scale Data, Mon Weather Rev, 118, 1250–1277, https://doi.org/10.1175/1520-0493(1990)118<1250:UOFDDA>2.0.CO;2, 1990.

Tarolli, P., Wang, W., Pijl, A., Cucchiaro, S., and Straffelini, E.: Heroic viticulture: Environmental and socioeconomic challenges of unique heritage landscapes, iScience, 26, 107125, https://doi.org/10.1016/j.isci.2023.107125, 2023.

Teslić, N.: Climate change vs Wine industry in the Emilia-Romagna : Assessment of the climate change , influence on wine industry and mitigation techniques, 2018.

Tonietto, J. and Carbonneau, A.: A multicriteria climatic classification system for grape-growing regions worldwide, Agric For Meteorol, 124, 81–97, https://doi.org/10.1016/j.agrformet.2003.06.001, 2004.

Tóth, J. P. and Végvári, Z.: Future of winegrape growing regions in Europe, Aust J Grape Wine Res, 22, 64–72, https://doi.org/10.1111/ajgw.12168, 2016.

Tradowsky, J. S., Philip, S. Y., Kreienkamp, F., Kew, S. F., Lorenz, P., Arrighi, J., Bettmann, T., Caluwaerts, S., Chan, S. C., De Cruz, L., de Vries, H., Demuth, N., Ferrone, A., Fischer, E. M., Fowler, H. J., Goergen, K., Heinrich, D., Henrichs, Y., Kaspar, F., Lenderink, G., Nilson, E., Otto, F. E. L., Ragone, F., Seneviratne, S. I., Singh, R. K., Skålevåg, A., Termonia, P., Thalheimer, L., van Aalst, M., Van den Bergh, J., Van de Vyver, H., Vannitsem, S., van Oldenborgh, G. J., Van Schaeybroeck, B., Vautard, R., Vonk, D., and Wanders, N.: Attribution of the heavy rainfall events leading to severe flooding in Western Europe during July 2021, Clim Change, 176, 90, https://doi.org/10.1007/s10584-023-03502-7, 2023.

Tramblay, Y. and Somot, S.: Future evolution of extreme precipitation in the Mediterranean, Clim Change, 151, 289–302, https://doi.org/10.1007/S10584-018-2300-5/FIGURES/4, 2018.

Trought, M. C. T., Howell, G. S., and Cherry, N.: Practical Considerations for Reducing Frost Damage in Vineyards, Report to New Zealand Winegrowers: 1999, 1–43, 1999.

Tuel, A. and Eltahir, E. A. B.: Why Is the Mediterranean a Climate Change Hot Spot?, J Clim, 33, 5829–5843, https://doi.org/10.1175/JCLI-D-19-0910.1, 2020.

Ugaglia, A. A., Cardebat, J.-M., and Corsi, A.: The Palgrave Handbook of Wine Industry Economics, edited by: Alonso Ugaglia, A., Cardebat, J.-M., and Corsi, A., Springer International Publishing, Cham, 47–77 pp., https://doi.org/10.1007/978-3-319-98633-3, 2019.

Wassennan, L. A.: All of Statistics A Concise Course in Statistical Inference, 2nd ed., Springer Nature; , 209–226 pp., 2004.

Welch, B. L.: The Significance of the Difference Between Two Means when the Population Variances are Unequal, Biometrika, 29, 350–362, https://doi.org/10.2307/2332010, 1938.

Zittis, G., Bruggeman, A., and Lelieveld, J.: Revisiting future extreme precipitation trends in the Mediterranean, Weather Clim Extrem, 34, https://doi.org/10.1016/j.wace.2021.100380, 2021.

Appendix A

Table A 1: Results of Welch's *t*-test applied to regional and consortia productivity data: *t* statistics (*t*), reference value for *t* (t_{ref}) and degrees of freedom (*DoF*) for the *t*-test based on the number of observations computed according to the Welch's equation for effective degrees of freedom (Welch, 1947) are displayed. Values of *t* lower than t_{ref} indicate that consortium and regional productivity samples comes from the same population, at 95% level of confidence. In the last column: temporal correlation coefficient (*r*) computed between consortium and regional productivity data. Asterisks (*) indicate statistically significant correlations (p<=0.05).

	t	t_{ref}	*DoF*	*r*
FRA vs LOM	1.17	2.01	47.94	0.62*
MON vs TOS	0.1	2	63.99	0.55*

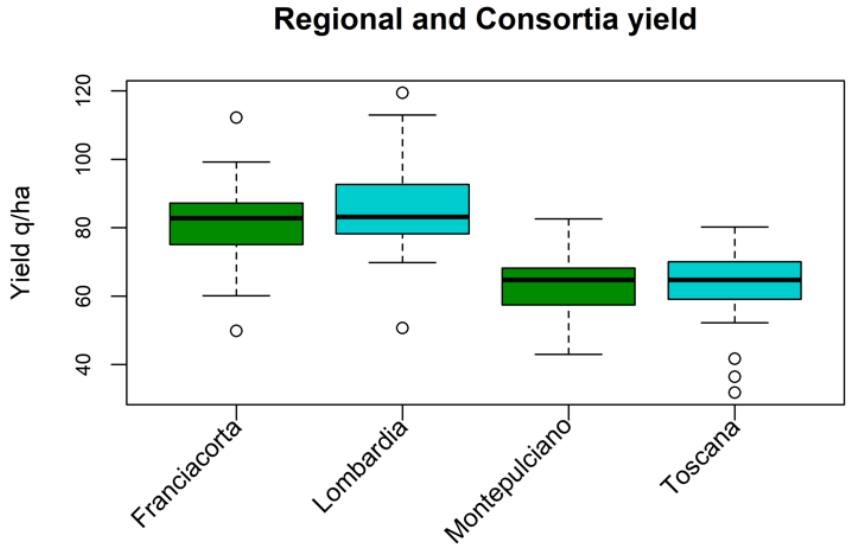

Figure A 1: Boxplots of regional (cyan) and consortia (green) productivity. The series of LOM and TOS come from ISTAT database and cover the period 1980-2019, with a six-year gap between 2000-2005, the period available for FRA is 1997-2019 (calculated by aggregating the Franciacorta DOCG and Curtefranca DOC denominations) and for MON is 1989-2019 (calculated by aggregating the Vino Nobile and Rosso di Montepulciano denominations), with no gap in the series.

Table A 2: Spearman correlation coefficient (ρ) , the root mean squared error (RMSE) between SPHERA (E-OBS) and CPM, as well as SPHERA (E-OBS) and RCM time series and the Normalised Root Mean Square Error (NRMSE) respect the range of values (y_{max} - y_{min}) of the reference (SPHERA and E-OBS) in FRA and MON area. Asterisks (*) indicate statistically significant correlations (p<=0.05).

FRA												
	TM			TX			TN			P		
	ρ	RMSE (°C)	NRMSE	ρ	RMSE (°C)	NRMSE	ρ	RMSE (°C)	NRMSE	ρ	RMSE (mm)	NRMSE
SPHERA vs CPM	0.95*	0.78	0.41	0.94*	1.54	0.74	0.96*	0.39	0.21	0.84*	233.52	0.25

SPHERA vs RCM	0.95*	0.38	0.2	0.96*	1.73	0.83	0.91*	1.37	0.74	0.73*	415.05	0.45
E-OBS vs CPM	0.76*	0.64	0.46	0.78*	0.6	0.22	0.55*	0.78	0.42	0.76*	435.99	0.68
E-OBS vs RCM	0.85*	0.37	0.27	0.82*	0.43	0.16	0.58*	0.61	0.33	0.77*	266.65	0.41
MON												
	TM			TX			TN			P		
	ρ	RMSE (°C)	NRMSE	ρ	RMSE (°C)	NRMSE	ρ	RMSE (°C)	NRMSE	ρ	RMSE (mm)	NRMSE
SPHERA vs CPM	0.79*	1.06	0.55	0.94*	1.54	0.48	0.96*	0.39	0.31	0.84*	233.52	0.35
SPHERA vs RCM	0.86*	0.91	0.48	0.96*	1.73	0.7	0.91*	1.37	0.41	0.73*	415.05	0.24
E-OBS vs CPM	0.16	0.79	0.28	0.78*	0.6	0.28	0.55*	0.78	0.5	0.76*	435.99	0.36
E-OBS vs RCM	0.06	0.83	0.29	0.82*	0.43	0.19	0.58*	0.61	0.34	0.77*	266.65	0.26

Table A 3: Results of Welch's *t*-test applied to mean (TM), maximum (TX) and minimum (TN) temperatures and precipitation (P) from E-OBS, SPHERA, RCM and CPM datasets, for FRA and MON: *t* statistics (*t*), reference value for *t* (t_{ref}), degrees of freedom (*DoF*) for the *t*-test based on the number of observations computed according to the Welch's equation for effective degrees of freedom (Welch, 1947) are displayed. Values of *t* higher than t_{ref} indicate that the samples from climate model simulations and the reference datasets come from different populations, at 95% level of confidence. Asterisks (*) indicate the means showing statistically significant differences.

FRA												
	SPHERA vs CPM			SPHERA vs RCM			E-OBS vs CPM			E-OBS vs RCM		
	t	t_{ref}	*DoF*	*t*	t_{ref}	*DoF*	*t*	t_{ref}	*DoF*	*t*	t_{ref}	*DoF*
TM	4.16*	2.03	35.2	1.8	2.03	34.77	2.98*	2.03	33.1	0.5	2.04	32.45
TX	6.7*	2.03	34.25	7.77*	2.03	34.83	-1.54	2.03	35.76	-0.75	2.03	35.95
TN	-2.31*	2.03	35.96	-8.26*	2.03	35.59	3.84*	2.03	36	-2.24*	2.03	35.83
P	-2.07*	2.03	35.85	-4.48*	2.03	35.47	4.93*	2.04	29.22	2.91*	2.04	32.58
MON												
	SPHERA vs CPM			SPHERA vs RCM			E-OBS vs CPM			E-OBS vs RCM		
	t	t_{ref}	*DoF*	*t*	t_{ref}	*DoF*	*t*	t_{ref}	*DoF*	*t*	t_{ref}	*DoF*
TM	6.45*	2.03	35.57	5.72*	2.03	35.03	-0.24	2.04	30.12	-0.95	2.04	29.09
TX	5.24*	2.03	35.97	8.15*	2.03	35.83	-3.29*	2.03	35.99	-0.81	2.03	35.76
TN	3.38*	2.04	32.37	-4.8*	2.04	32.12	4.89*	2.06	24.89	-0.87	2.06	24.71
P	2.33*	2.03	35.69	1.3	2.03	35.91	2.37*	2.03	35.57	1.34	2.03	35.96

Table A 4: Results of Welch's *t*-test applied to the bioclimatic indices from E-OBS, SPHERA, RCM and CPM datasets, for FRA and MON: *t* statistics (*t*), reference value for *t* (t_{ref}), degrees of freedom (*DoF*) for the *t*-test based on the number of observations computed according to the Welch's equation for effective degrees of freedom (Welch, 1947) are displayed. Values of *t* higher than t_{ref} indicate that the samples from climate model simulations and the reference datasets come from different populations, at 95% level of confidence. Asterisks (*) indicate the means showing statistically significant differences.

FRA												
	SPHERA vs CPM			SPHERA vs RCM			E-OBS vs CPM			E-OBS vs RCM		
Index	*t*	t_{ref}	*DoF*	*t*	t_{ref}	*DoF*	*t*	t_{ref}	*DoF*	*t*	t_{ref}	*DoF*
BEDD (GDD)	-0.92	2.03	35.97	-0.17	2.03	35.97	0.67	2.03	35.36	1.47	2.03	35.35
HI (GDD)	-4.50*	2.04	32.50	-4.71*	2.03	33.34	-0.88	2.04	32.14	-0.96	2.03	33.01
WI (GDD)	-4.48*	2.04	32.68	-4.13*	2.04	32.65	-3.25*	2.04	30.29	-2.89*	2.04	30.26
TmVeg (°C)	-4.59*	2.04	32.60	-4.17*	2.04	32.59	-3.28*	2.04	30.54	-2.85*	2.04	30.53
TnVeg (°C)	2.86*	2.03	32.92	5.35*	2.03	35.87	-0.16	2.04	30.41	2.42*	2.03	34.63
TxVeg (°C)	-8.32*	2.03	32.82	-8.62*	2.03	35.95	-5.47*	2.04	30.10	-5.30*	2.03	34.76
CNI (°C)	0.99	2.03	33.37	2.29*	2.03	35.16	-1.22	2.03	33.70	-0.11	2.03	35.37
TnRest	-0.23	2.03	35.51	2.69*	2.03	35.40	-2.53*	2.03	35.77	0.15	2.03	35.84
GSP (mm)	5.55*	2.03	35.93	8.76*	2.03	33.94	-4.23*	2.04	32.17	-1.48	2.03	35.20
SprR (mm)	-0.03	2.03	36.00	1.92	2.03	35.18	-3.80*	2.04	31.84	-1.86	2.03	34.38
MON												
	SPHERA vs CPM			SPHERA vs RCM			E-OBS vs CPM			E-OBS vs RCM		
Index	*t*	t_{ref}	*DoF*	*t*	t_{ref}	*DoF*	*t*	t_{ref}	*DoF*	*t*	t_{ref}	*DoF*
BEDD (GDD)	-2.25*	2.03	35.88	-2.13*	2.03	35.84	1.91	2.03	34.16	2.04*	2.03	34.04
HI (GDD)	-3.31*	2.03	34.11	-3.71*	2.03	35.41	-1.37	2.03	33.35	-1.65	2.03	34.90
WI (GDD)	-5.21*	2.03	34.38	-5.66*	2.03	35.53	-2.14*	2.03	36.00	-2.37*	2.03	35.56
TmVeg (°C)	-5.38*	2.03	34.59	-5.79*	2.03	35.61	-2.06*	2.03	35.96	-2.24*	2.03	35.38
TnVeg (°C)	-0.54	2.03	35.91	2.90*	2.03	35.78	-1.35	2.03	33.90	1.70	2.03	33.44
TxVeg (°C)	-5.43*	2.03	35.98	-5.36*	2.03	35.06	-3.74*	2.03	35.86	-3.57*	2.03	34.60
CNI (°C)	-1.61	2.03	33.38	0.98	2.03	34.58	-3.31*	2.03	34.96	-0.92	2.03	35.70
TnRest	-2.27*	2.03	35.17	-0.82	2.03	34.45	-2.35*	2.03	33.56	-1.01	2.04	32.57
GSP (mm)	-1.05	2.04	31.29	2.46*	2.03	35.02	-3.06*	2.05	26.93	-0.04	2.03	35.74
SprR (mm)	-2.44*	2.05	27.64	-0.44	2.04	31.33	-2.75*	2.04	32.09	-0.95	2.03	35.18

Table A 5: Sen's slope estimator, a statistical measure to evaluate the magnitude of the trend, for FRA area. Asterisk (*) indicate a significant trend (p<=0.05).

FRA	TM (°C/yr)	TX (°C/yr)	TN (°C/yr)	P (mm/yr)	BEDD (GDD/yr)	HI (GDD/yr)	WI (GDD/yr)	TmVeg (°C/yr)	TnVeg (°C/yr)	TxVeg (°C/yr)	CNI (°C/yr)	TnRest (°C/yr)	GSP (mm/yr)	SprR (mm/yr)
E-OBS	0.05*	0.05	0.06*	-5.91	4.59*	14.96*	11.67	0.06*	0	0.1	0.09	0.03	-4.77	-1.33
SPHERA	0.04	0.03	0.04*	12.89	4.5	9.25	6.65	0.04	0.02	0.05	0.1	0.02	13.32*	4.57*
CPM	0.04	0.03	0.04	6.54	3.35	13.34	12.61	0.06	0.01	0.12	0.13*	0.05	-1.31	0.7
RCM	0.05*	0.04	0.04*	-2.14	4.19	11.51	11.94	0.06	0.05*	0.12*	0.12	0.07	-2.41	-0.15

Table A 6: Sen's slope estimator, a statistical measure to evaluate the magnitude of the trend, for MON area. Asterisk (*) indicate a significant trend (p<=0.05).

MON	TM (°C/yr)	TX (°C/yr)	TN (°C/yr)	P (mm/yr)	BEDD (GDD/yr)	HI (GDD/yr)	WI (GDD/yr)	TmVeg (°C/yr)	TnVeg (°C/yr)	TxVeg (°C/yr)	CNI (°C/yr)	TnRest (°C/yr)	GSP (mm/yr)	SprR (mm/yr)
E-OBS	-0.07*	0.04	-0.11*	8.64	-7.89*	1.23	-17.42*	-0.08*	-0.09	0.07	-0.07	0.03	4.38	0.07

SPHERA	0.03	0.01	0.03*	19.47*	2.94	5.05	7.22	0.03	0.1*	-0.08*	0.12*	0	10.36*	0.99
CPM	0.03	0.02	0.03*	5.28	2.42	6.84	3.68	0.02	0.05*	0.05*	0.15	0	0.74	1
RCM	0.04	0.03	0.03*	6.28	1.2	10.5	9.31	0.04	0.06*	0.01	0.11*	0.06	-0.08	0.34

Table A 7: Sen's slope of the productivity in FRA and MON. Sen's slope is a statistical measure used to calculate the rate of change in a variable over time, based on the Sen's estimator. Asterisk (*) indicate a significant trend (p<=0.05)

Consortium	Productivity (q/ha)/yr
FRA	1.28*
MON	0.43

Table A 8: ranking of the maximum variance (%) explained for each dataset for each consortium, with the indication of type of method used (SR: single regression, MR multiple regression.)

FRA			MON		
Model	var.value %	type	Model	var.value %	type
RCM	64 %	MR	CPM	45 %	MR
SPHERA	56 %	MR	E-OBS	44 %	SR
CPM	48 %	MR	SPHERA	42 %	MR
E-OBS	42 %	SR	CPM	34 %	SR
SPHERA	36 %	SR	RCM	32 %	SR
E-OBS	35 %	MR	E-OBS	32 %	MR
RCM	35 %	SR	RCM	29 %	MR
CPM	34 %	SR	SPHERA	21 %	SR